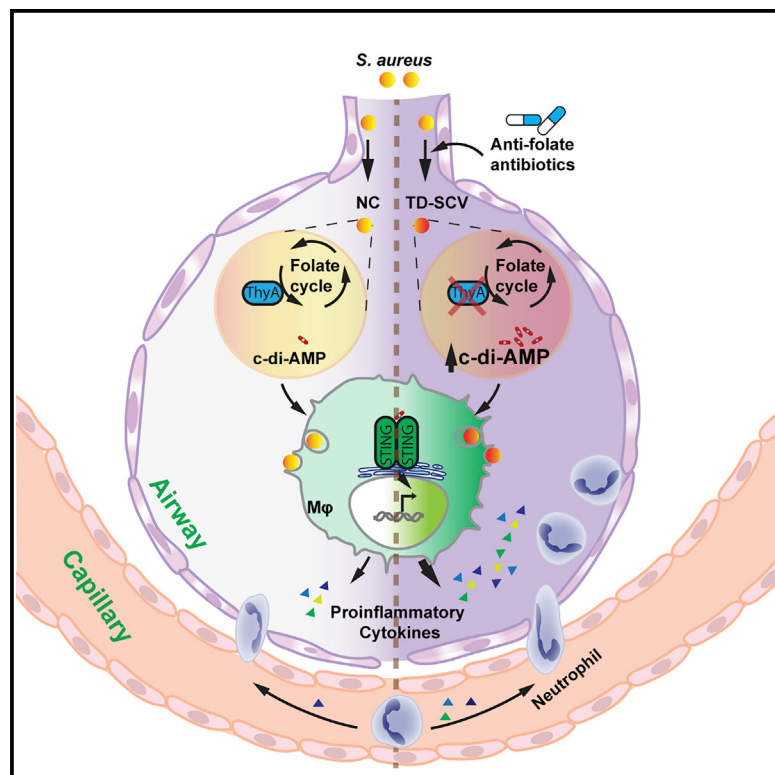


Thymidine starvation promotes c-di-AMP-dependent inflammation during pathogenic bacterial infection

Graphical abstract



Authors

Qing Tang, Mimi R. Precit,
Maureen K. Thomason,,
Daniel J. Wolter, Lucas R. Hoffman,
Joshua J. Woodward

Correspondence

jjwoodwa@uw.edu

In brief

Tang et al. find that disruption of thymidine biosynthesis by antifolate antibiotics induce elevated c-di-AMP production of many pathogenic Firmicutes species, which consequently leads to higher STING activation. This study reveals an unappreciated link between antibiotic therapy and host inflammation.

Highlights

- Disruption of thymidine biosynthesis elevates c-di-AMP production in many Firmicutes
- S. aureus* thymidine-dependent SCVs (TD-SCVs) produce excessive c-di-AMP
- Elevated c-di-AMP produced by TD-SCVs induces robust STING activation in cells
- TD-SCV infection leads to higher airway inflammation compared with normal colony (NC)

Article

Thymidine starvation promotes c-di-AMP-dependent inflammation during pathogenic bacterial infection

Qing Tang,¹ Mimi R. Precit,¹ Maureen K. Thomason,¹ Sophie F. Blanc,¹ Fariha Ahmed-Qadri,¹ Adelle P. McFarland,¹ Daniel J. Wolter,^{2,3} Lucas R. Hoffman,^{1,2,3} and Joshua J. Woodward^{1,4,*}

¹Department of Microbiology, University of Washington, Seattle, WA 98105, USA

²Department of Pediatrics, University of Washington, Seattle, WA 98105, USA

³Pulmonary and Sleep Medicine, Seattle Children's Hospital, Seattle, WA 98105, USA

⁴Lead contact

*Correspondence: jjwoodwa@uw.edu

<https://doi.org/10.1016/j.chom.2022.03.028>

SUMMARY

Antimicrobials can impact bacterial physiology and host immunity with negative treatment outcomes. Extensive exposure to antifolate antibiotics promotes thymidine-dependent *Staphylococcus aureus* small colony variants (TD-SCVs), commonly associated with worse clinical outcomes. We show that antibiotic-mediated disruption of thymidine synthesis promotes elevated levels of the bacterial second messenger cyclic di-AMP (c-di-AMP), consequently inducing host STING activation and inflammation. An initial antibiotic screen in Firmicutes revealed that c-di-AMP production was largely driven by antifolate antibiotics targeting dihydrofolate reductase (DHFR), which promotes folate regeneration required for thymidine biosynthesis. Additionally, TD-SCVs exhibited excessive c-di-AMP production and STING activation in a thymidine-dependent manner. Murine lung infection with TD-SCVs revealed STING-dependent elevation of proinflammatory cytokines, causing higher airway neutrophil infiltration and activation compared with normal-colony *S. aureus* and hemin-dependent SCVs. Collectively, our results suggest that thymidine metabolism disruption in Firmicutes leads to elevated c-di-AMP-mediated STING-dependent inflammation, with potential impacts on antibiotic usage and infection outcomes.

INTRODUCTION

The discovery of antibiotics over 100 years ago marked one of the most significant advancements in human medical interventions of the 20th century. The widespread acquisition of antibiotic resistance has continuously challenged antibiotic utility, necessitating the continued development of new antimicrobial classes that disrupt distinct aspects of bacterial physiology. *In vitro*, these compounds inhibit microbial growth or directly kill microbes, depending upon their mechanism of action. In the *in vivo* context, these therapeutic agents can directly affect the host immune system—in many cases, augmenting microbial growth inhibition and in some instances, leading to pathological inflammation, most notably toxic shock (Anderson et al., 2010). Despite decades of study, the complex relationship between antimicrobials, bacterial physiology, and host immunity remains incompletely understood.

Cyclic dinucleotides (CDNs) of bacterial origin mediate host immune responses to infection. Cyclic di-AMP (c-di-AMP) released by bacteria during infection serves as a conserved microbial signature for innate immune detection of several pathogens (Woodward et al., 2010). The host protein STING (stimulator of interferon genes) binds bacterial CDNs (c-di-AMP, c-di-GMP, and 3'3'-cGAMP), in addition to eukaryotic 2'3'-cGAMP, which

is synthesized by cyclic GMP-AMP synthase (cGAS) in response to host or pathogen DNA (Burdette et al., 2011; Ishikawa and Barber, 2008; Sun et al., 2013; Wu et al., 2013; Zhang et al., 2013). STING binding to CDNs promotes IRF3 phosphorylation and translocation to the nucleus to mediate transcription of IFN- β and other coregulated genes (Burdette et al., 2011). Additionally, STING activation promotes NF- κ B, MAP kinase, STAT6, NLRP3 inflammasome activation, apoptosis, and autophagy, independent of IFN- β (Balka et al., 2020; Chen et al., 2011; Gaidt et al., 2017; Gui et al., 2019; Gulen et al., 2017). Collectively, the CDN-STING signaling axis has emerged as a central mediator of host immunity to microbial infection in a variety of contexts (Cheng et al., 2020; Ma and Damania, 2016; Sun and Cheng, 2020). Aberrant STING activation results in the development of several autoimmune disorders affecting the brain, vasculature, and lungs (Frémont et al., 2021; Gao et al., 2015; Liu et al., 2014). It is currently unclear if STING activation is impacted by antimicrobial treatment or how such treatment impacts infection outcome.

Many mechanisms of antibiotic resistance have been documented in both clinical and laboratory settings. In many organisms, including *Staphylococcus aureus*, antibiotic therapy can drive the emergence of isolates harboring disruptions in genes involved in fundamental metabolic pathways. The resulting small

colony variants (SCVs) exhibit slow *in vitro* growth and are associated with antibiotic-refractory, chronic infections, including osteomyelitis, endocarditis, wound infections, and lung infections in patients with the autosomal recessive disease cystic fibrosis (CF) (Goerke and Wolz, 2010; Proctor et al., 2006). As such, SCV infections are difficult to eradicate and can persist for many years. The second messenger c-di-AMP plays a pleiotropic role in bacterial stress responses by impacting cell wall synthesis, osmolyte level regulation, DNA damage repair, and cell wall-targeting antibiotic resistance (Stülke and Krüger, 2020; Yin et al., 2020). Accumulation of c-di-AMP by mutation of the phosphodiesterase GdpP mediates β-lactam resistance in clinical isolates of *S. aureus* (Aragudín et al., 2018; Ba et al., 2019; Sommer et al., 2021). Despite our understanding of c-di-AMP function in microbial physiology, the impact of this signaling molecule on the central processes disrupted by antibiotic exposure and those involved in antibiotic resistance is poorly defined.

In this study, the impacts of antibiotic exposure on STING-dependent inflammation and c-di-AMP production were assessed. Elevated c-di-AMP production and STING-dependent inflammation following the disruption of thymidine metabolism were observed among several pathogens. *S. aureus* SCVs carrying mutations in the enzyme thymidylate synthase confer similar c-di-AMP and STING-dependent hyperinflammation and elevated inflammatory cell recruitment to the airway during infection of the lung. Collectively, these findings reveal an unappreciated link between antibiotic therapy, antifolate resistance, and host inflammation, providing initial insight into how these processes impact host outcomes during infection.

RESULTS

Antibiotic stresses contribute to bacterial intracellular c-di-AMP accumulation

In many Firmicutes, c-di-AMP mediates microbial stress responses and viability in several growth conditions (Stülke and Krüger, 2020). However, there remains a dearth of knowledge pertaining to the environmental cues that impact nucleotide dynamics in this phylum of bacteria. Given that antibiotics target central aspects of bacterial physiology, we hypothesized that exposure to these therapeutic agents could modulate nucleotide levels and illuminate c-di-AMP's role in central microbial stress responses.

The intracellular pathogen *Listeria monocytogenes* secretes c-di-AMP, which activates STING and elicits IFN-β production (Woodward et al., 2010), providing an indirect readout of c-di-AMP during infection. We performed a screen by incubating *L. monocytogenes* in BIOLOG microplates (PM11C and PM12B) containing 48 different antibiotics at various concentrations. Bacteria were subsequently used to infect primary murine bone marrow-derived macrophages (pBMDMs), and IFN-β production was measured by ISRE-luciferase bioassay. *L. monocytogenes* treated with β-lactam antibiotics induced elevated IFN-β concentrations relative to the untreated control (Figure 1A). Unexpectedly, we observed elevation of IFN-β following exposure to the antifolate 2,4-diamino-6,7-diisopropylpteridine (Figures 1A and 1B). To validate and expand upon these observations, *L. monocytogenes* was treated with other antifolates, including sulfamethoxazole, trimethoprim, and SXT

(trimethoprim/sulfamethoxazole combination in a 1:5 ratio, also known as Bactrim), as well as the cell wall inhibitor penicillin G. Consistent with the initial screen, penicillin G-induced elevated IFN-β production during *L. monocytogenes* infection. Additionally, antibiotics targeting dihydrofolate reductase (DHFR), which converts dihydrofolate to tetrahydrofolate, induced significantly higher IFN-β production, whereas treatment with the dihydopteroate synthase (DHPS) inhibitor sulfamethoxazole, an enzyme involved in dihydrofolate synthesis, resulted in a comparable level of IFN-β relative to the untreated control (Figure 1C). These observations reveal that antibiotics that target tetrahydrofolate synthesis promote IFN-β production during infection by *L. monocytogenes*.

In the absence of antibiotics, IFN-β production during *L. monocytogenes* infection is primarily attributed to the direct activation of STING by bacterial c-di-AMP. However, IFN-β production can also result from activation of cGAS by host- or pathogen-derived DNA and subsequent 2'3'-cGAMP-mediated STING activation (Wu et al., 2013) (Figure 1D). To discriminate between direct bacterial STING antagonism or bacterial DNA release, WT, *Sting*^{-/-}, and *cGas*^{-/-} pBMDMs were infected with *L. monocytogenes* cultured with or without a subinhibitory concentration of SXT. In both cases, *Ifnb1* induction was greatly reduced in the absence of STING, and there was an insignificant effect of SXT on *Ifnb1* expression, confirming the role of this CDN receptor, regardless of antibiotic presence (Figure 1E). Additionally, SXT-treated *L. monocytogenes* induced significantly higher *Ifnb1* transcription in both WT and *cGas*^{-/-} cells relative to the untreated control (Figure 1E). Because antibiotic-induced *Ifnb1* expression was cGAS independent, these observations support direct STING activation by *L. monocytogenes* following SXT exposure.

Our findings suggested that exposure to antibiotics that target DHFR results in increased CDN production. To confirm this assertion, we monitored c-di-AMP levels in *L. monocytogenes* treated with penicillin G, 2,4-diamino-6,7-diisopropylpteridine, sulfamethoxazole, trimethoprim, and SXT. c-di-AMP levels directly mirrored the IFN-β induction observed following macrophage infection (Figure 1F). Collectively, these observations reveal that antibiotics that target DHFR result in elevated c-di-AMP production by *L. monocytogenes*, which promote STING-dependent IFN-β production by infected host cells.

Thymidine deficiency promotes c-di-AMP production of Firmicutes

DHFR plays a key role in folate regeneration required for *de novo* biosynthesis of thymidine, amino acids, and purines (Hawser et al., 2006). The bactericidal activity of antifolates is attributed to disrupted thymidine synthesis and subsequent thymineless death (Fernández-Villa et al., 2019). Therefore, we quantified bacterial c-di-AMP levels as well as macrophage IFN-β production during infection with *L. monocytogenes* grown under SXT stress in the presence or absence of exogenous thymidine. In the absence of thymidine, SXT induced a 15-fold elevation of c-di-AMP and IFN-β production, whereas thymidine supplementation complemented c-di-AMP and IFN-β levels induced by SXT exposure (Figures 2A and 2B). These observations indicated that elevated c-di-AMP levels following DHFR inhibition result from disruption of thymidine biosynthesis. To further verify this indication, we generated an in-frame deletion of the thymidylate

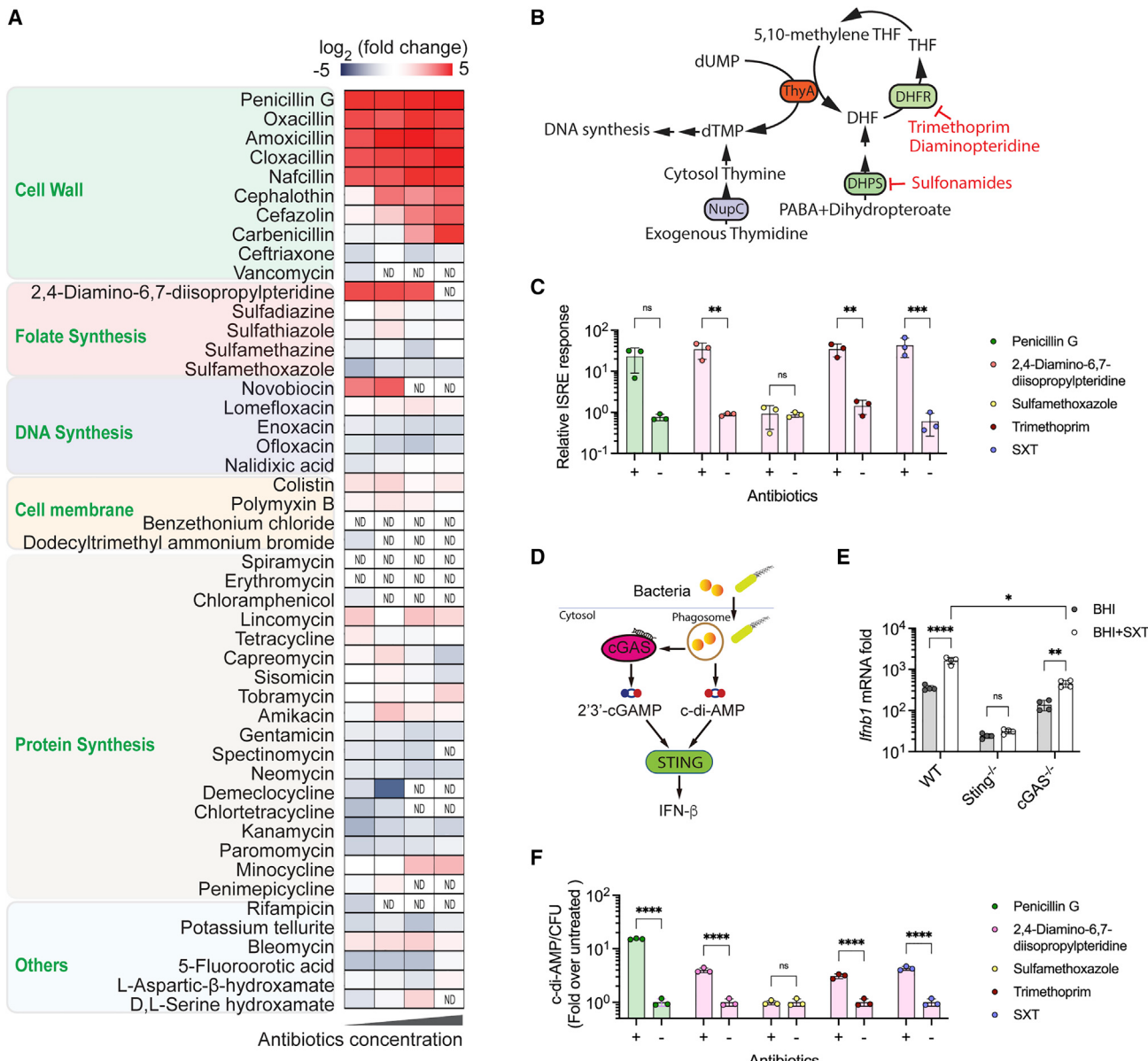


Figure 1. Antibiotic treatment promotes c-di-AMP production by bacteria

(A) Heatmap of relative IFN- β production in pbMDMs infected with *L. monocytogenes* incubated in BIOLOG antibiotic plates as measured by ISRE-luciferase bioassays. The log₂ ratios of IFN- β relative to untreated *L. monocytogenes* are shown. Black labels indicate different antibiotics, green labels indicate the antibiotic class based on mechanism of action. ND indicates that no bacteria were recovered after treatments, and IFN- β was not determined.

(B) Schematic of thymidine metabolism in bacteria. ThyA, thymidylate synthase; NupC, nucleoside permease; DHFR, dihydrofolate reductase; and DHPS, dihydropteroate synthase.

(C) IFN- β production of pBMDMs infected with *L. monocytogenes* treated with indicated antibiotics relative to the untreated control at 6 hpi as measured by ISRE-luciferase bioassays. Logarithmic-phase *L. monocytogenes* were incubated with either 15 μ g/mL penicillin G, 200 μ g/mL 2,4-diamino-6,7-diisopropylpteridine, 1,200 μ g/mL sulfamethoxazole, 250 μ g/mL trimethoprim, or 50 μ g/mL SXT for 6 h before macrophage phagocytosis.

(D) Schematic of STING activation. Eukaryotic 2'3'-cGAMP synthesized by cGAS in response to host- or pathogen-derived DNA, and bacterial cyclic dinucleotides can both activate STING, resulting in IFN- β induction.

(E) *Ifnb1* mRNA expression in WT, *Sting*^{-/-} or *cGas*^{-/-} pBMDMs infected with *L. Monocytogenes* grown in BHI broth with or without 0.25 µg/mL of SXT supplementation at 4 hpi.

(F) Quantification of intracellular c-di-AMP production of *L. monocytogenes* treated with antibiotics as indicated in (C) using CDA-Luc assay. For all panels, mean values of biological replicates are plotted, and error bars indicate \pm SD. p values were calculated using two-way ANOVA analysis. Asterisks indicate statistical significance (*, $p < 0.05$; **, $p < 0.01$; ***, $p < 0.001$, ****, $p < 0.0001$), and ns indicates no significant difference.

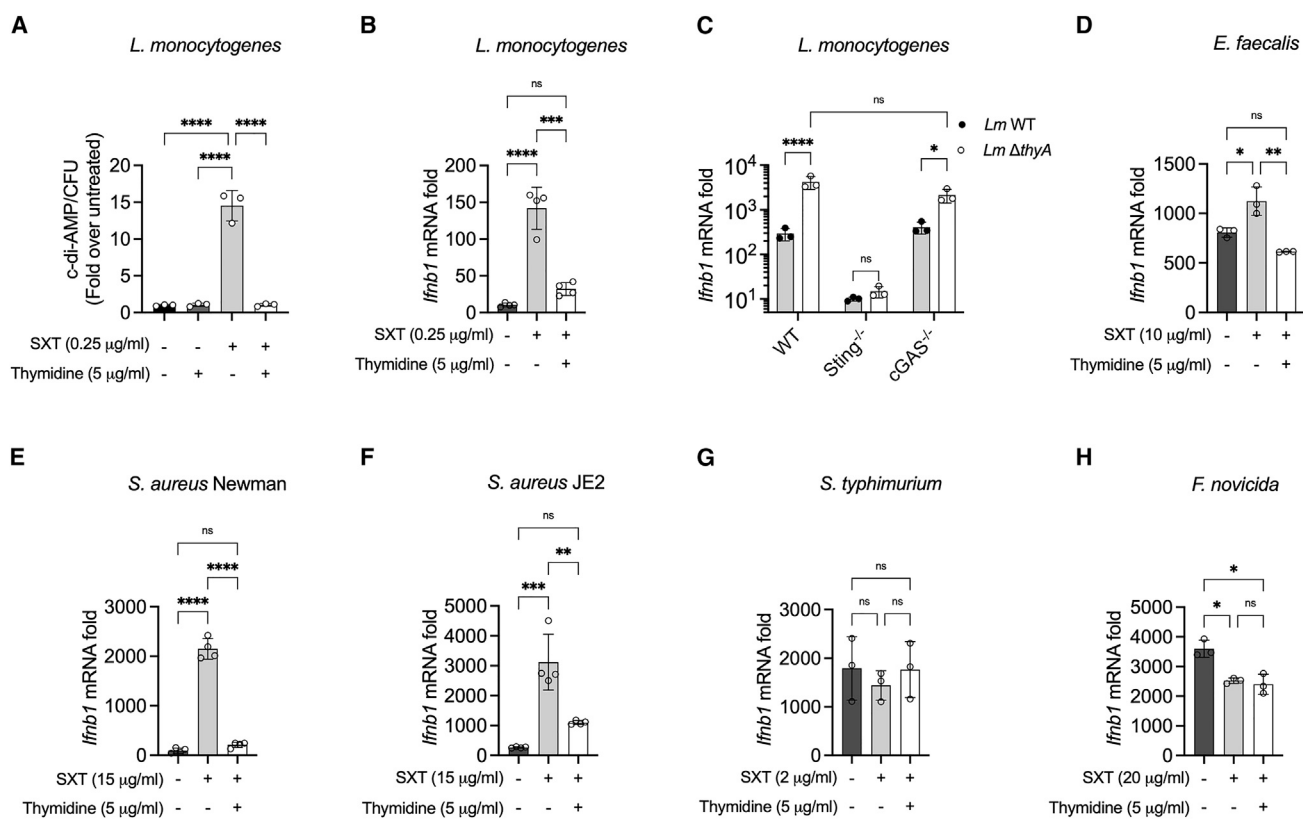


Figure 2. *L. monocytogenes* ThyA inhibition or mutation leads to higher c-di-AMP production

(A) Intracellular c-di-AMP concentration of *L. monocytogenes* grown in BHI broth with indicated SXT and thymidine supplementation quantified by CDA-Luc assay.

(B) *Ifnb1* mRNA induction in pBMDMs infected with *L. monocytogenes* grown in BHI broth as indicated in (A).

(C) *Ifnb1* mRNA induction by WT or *ΔthyA* *L. monocytogenes* strains in WT, *Sting*^{-/-}, or *cGAS*^{-/-} pBMDMs at 4 hpi.

(D–H) *Ifnb1* mRNA induction in pBMDMs infected with either *E. faecalis* (D), *S. aureus* Newman (E), *S. aureus* JE2 (F), *S. typhimurium* (G), or *F. novicida* (H) grown in the indicated conditions. For all panels, mean values of biological replicates are plotted, and error bars indicate \pm SD. p values were calculated using two-way ANOVA analysis. Asterisks indicate statistical significance (*, p < 0.05, **, p < 0.01; ****, p < 0.0001), and ns indicates no significant difference.

synthase gene *thyA* in *L. monocytogenes* and monitored *Ifnb1* induction during macrophage infection. Consistent with SXT treatment, *ΔthyA* induced significantly higher *Ifnb1* expression relative to WT *L. monocytogenes* in STING-dependent and cGAS-independent manners (Figure 2C). These observations support that altered thymidine biosynthesis, either through antifolate exposure or via genetic means, promotes c-di-AMP production by *L. monocytogenes*.

Although tetrahydrofolate is an essential cosubstrate for ThyA in all bacteria (Kompis et al., 2005), the diadenylate cyclase (DacA) that synthesizes c-di-AMP is essential for Firmicutes but is absent in most Proteobacteria (Stölke and Krüger, 2020). To explore the generality of our observations linking thymidine metabolism and IFN- β production during infection, four common human pathogens were grown under subinhibitory concentrations of SXT in the presence or absence of surplus exogenous thymidine, and induction of *Ifnb1* transcription was assessed by qRT-PCR following macrophage infection. SXT treatment induced *Ifnb1* expression in a thymidine-dependent (TD) manner in the c-di-AMP producing Firmicutes *Enterococcus faecalis* (Figure 2D), *S. aureus* Newman (Figure 2E), and *S. aureus* JE2

(Figure 2F). However, the c-di-AMP-deficient Proteobacteria *Salmonella enterica* serovar Typhimurium (Figure 2G) and *Francisella novicida* (Figure 2H) either induced comparable *Ifnb1* in all conditions or decreased *Ifnb1* after SXT treatment, regardless of thymidine supplementation. These results provide evidence that disrupting thymidine metabolism increases c-di-AMP production in diverse Firmicutes, but not among Proteobacteria that do not produce this second messenger.

S. aureus TD-SCVs activate STING signaling through c-di-AMP

SXT is widely used to treat various bacterial infections, including the pulmonary, skin, and soft-tissue infections caused by *S. aureus*. SXT use can result in the emergence of antifolate-resistant *S. aureus* (Besier et al., 2008a; Kriegeskorte et al., 2015), referred to as TD-SCVs. TD-SCVs are thymidine auxotrophs due to inactivating mutations in *thyA*, yielding nonhemolytic, small colonies when cultured on blood agar plates. Clinically, TD-SCVs are associated with chronic and recurring antibiotic-resistant infections. Notably, chronic respiratory infection with TD-SCVs are associated with a significantly increased risk of

Cell Host & Microbe

Article

CellPress

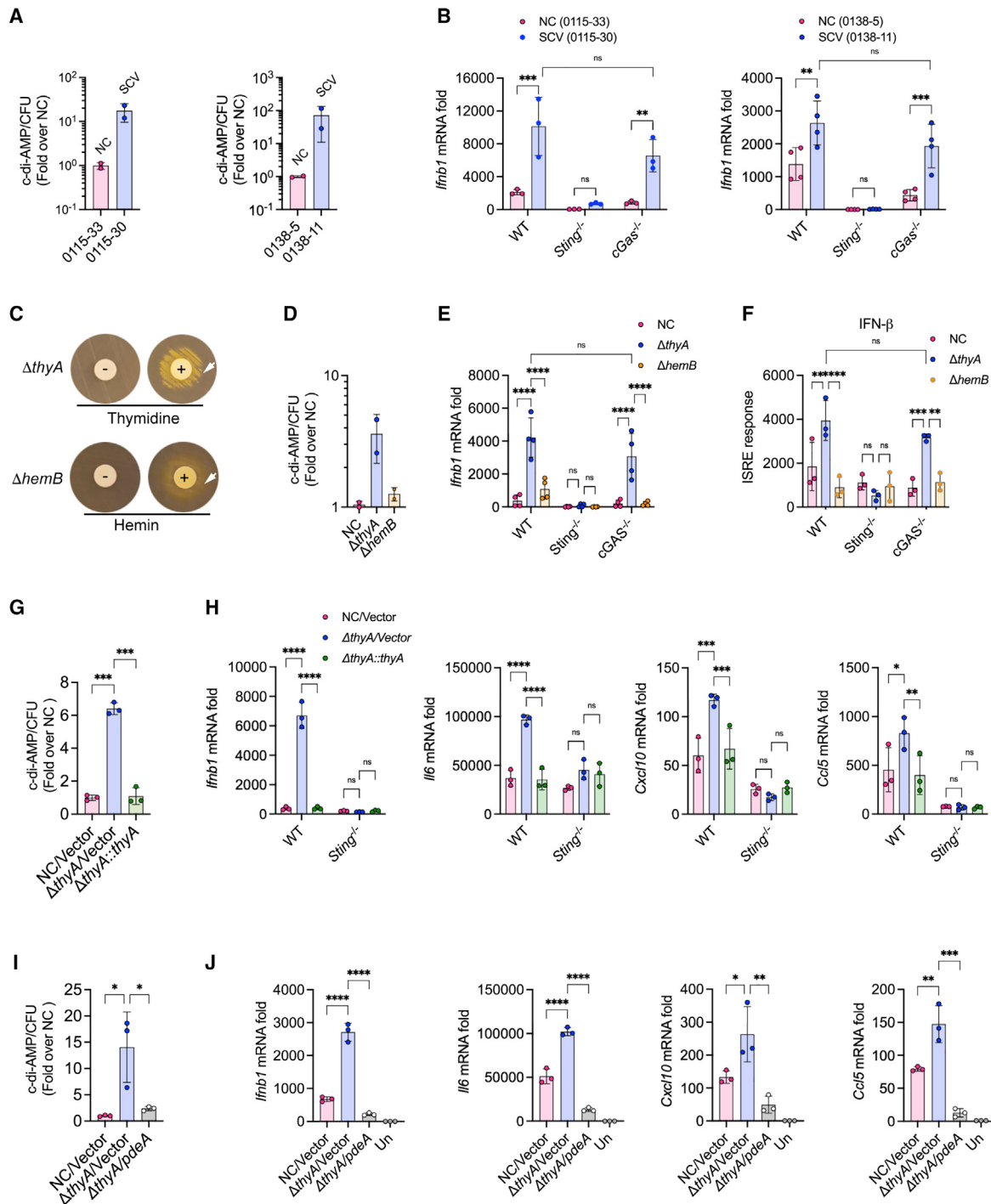


Figure 3. ΔthyA activates STING-dependent type I IFN production through c-di-AMP in primary macrophages

(A) LC-MS/MS quantification of c-di-AMP levels of clinical TD-SCV isolates (0115-30 and 0138-11) relative to clonally related normal-colony (NC) isolates (0115-33 and 0138-5) grown on chocolate agar overnight.

(B) Ifnb1 expression in pBMDMs infected with clinical isolates at 4 hpi relative to uninfected control.

(C) Auxotrophy test for thymidine and hemin dependence of ΔthyA or ΔhemB plated on Mueller-Hinton agar. Representative image shows enhanced growth, indicated by white arrows, around disks impregnated with thymidine or hemin.

(D) LC-MS/MS quantification of c-di-AMP levels of ΔthyA and ΔhemB relative to NC. Cultures of ΔthyA and ΔhemB were supplemented with 5 µg/mL of thymidine and 1 µg/mL hemin, respectively.

(E) Ifnb1 mRNA induction by NC, ΔthyA, and ΔhemB Newman strains in WT, Sting^{-/-}, and cGAS^{-/-} pBMDMs at 4 hpi relative to uninfected controls.

(legend continued on next page)

respiratory exacerbations and reduced lung function in patients with pediatric CF, whereas those with non-TD SCVs are not (Wolter et al., 2013, 2019). Although the link between TD-SCVs and worse lung disease is documented (Besier et al., 2007; Wolter et al., 2013, 2019), the mechanism behind these observations is not understood. We hypothesized that this clinical association resulted from increased inflammation induced by TD-SCV infections relative to other *S. aureus* isolates. We therefore further characterized the impacts of SXT and $\Delta thyA$ mutation on the dynamics of infection by *S. aureus* and resulting inflammation.

pBMDMs were infected with two sets of clonally related *S. aureus* normal-colony (NC) and SCV isolates collected during a study of children with CF (Precit et al., 2016). We found that the clinical TD-SCV isolates exhibited between 10- and 100-fold higher levels of c-di-AMP/CFU (Figure 3A) and simultaneously induced significantly higher *Ifnb1* in both WT and $cGas^{-/-}$ pBMDMs relative to NC clonal isolates (Figure 3B). These observations suggest that *S. aureus* TD-SCV clinical isolates induce elevated STING-dependent inflammation as a consequence of inactivating mutations in the *thyA* gene.

Our findings that clinical TD-SCVs induced elevated STING-dependent inflammation relative to clonally related NC isolates as a consequence of *thyA* mutations did not exclude the possibility that these clinical isolates might carry secondary mutations that could influence these results. We therefore generated an isogenic $\Delta thyA$ *S. aureus* Newman strain. Additionally, we constructed a hemin-dependent SCV (HD-SCV) strain containing a deletion in the porphobilinogen synthase gene *hemB* in *S. aureus* Newman to use as a SCV control. HD-SCVs are also observed during human infections, and although hemin-deficient SCVs exhibit slow growth rates and antibiotic resistance, they are not known to be associated with worse CF lung disease outcomes (Wolter et al., 2019).

Growth of $\Delta thyA$ and $\Delta hemB$ on indicator media was complemented by supplementation of exogenous thymidine or hemin, respectively (Figure 3C). At logarithmic phase, $\Delta thyA$ produced about 2-fold higher c-di-AMP than both NC and $\Delta hemB$ strains grown in BHI broth, even with surplus thymidine supplementation (5 µg/mL) (Figure 3D), which phenocopied the clinical TD-SCVs (Figure 3A). WT, $Sting^{-/-}$, and $cGas^{-/-}$ pBMDMs were infected with either NC, $\Delta thyA$, or $\Delta hemB$ *S. aureus* Newman strains, and intracellular bacterial survival was measured under each condition. NC and $\Delta hemB$ exhibited similar survival trends over 8 h post-infection (hpi), whereas $\Delta thyA$ exhibited significantly reduced persistence in all cell lines (Figure S1A). Additionally, all strains generated comparably low levels of macrophage toxicity, as assessed by lactate dehydrogenase (LDH) release (Figure S1B). Despite the diminished CFU burden, *S. aureus* $\Delta thyA$ induced elevated STING-dependent and cGAS-independent *Ifnb1* transcription and IFN- β levels than either NC or $\Delta hemB$ strains. *Ifnb1* induction by $\Delta thyA$ was abolished in $Sting^{-/-}$ pBMDMs but only

slightly diminished in $cGas^{-/-}$ pBMDMs (Figures 3E and 3F). Beyond *Ifnb1*, Taqman cytokine arrays in macrophages infected with TD-SCV also revealed significant elevation in the production of the *Ifnb1* coregulated genes *Il6*, *Cxcl10*, and *Ccl5* (Figures S2A–S2D), which are expressed upon activation of STING signaling (Abe and Barber, 2014; Balka et al., 2020; Yum et al., 2021).

Complementation of $\Delta thyA$ in *trans* with the *thyA* gene driven by its original promoter exhibited similar c-di-AMP production as the WT Newman strain (Figure 3G) and rescued the survival defect of $\Delta thyA$ within cells (Figure S1C). Furthermore, $\Delta thyA$ complementation rescued the higher expressions of *Ifnb1*, *Il6*, *Cxcl10*, and *Ccl5* in WT pBMDMs induced by $\Delta thyA$, whereas all bacterial strains exhibited comparable lower induction of these genes in $Sting^{-/-}$ pBMDMs (Figure 3H). These data further indicate that *thyA* deficiency leads to higher c-di-AMP production, which promotes the expression of STING-dependent immune genes.

To further verify that the STING activation upon $\Delta thyA$ infection is due to c-di-AMP, $\Delta thyA$ overexpressing the soluble fragment of *L. monocytogenes* PdeA, which is a c-di-AMP-specific phosphodiesterase that degrades c-di-AMP (Witte et al., 2013), was used for macrophage infections along with NC and $\Delta thyA$ strains. Consistent with our hypothesis, expression of the c-di-AMP phosphodiesterase in $\Delta thyA$ decreased its c-di-AMP concentration (Figure 3I) and simultaneously eliminated its induction of *Ifnb1* and coregulated genes (Figure 3J). Furthermore, heat killing of bacterial cells abolished c-di-AMP production and consequently blunted *Ifnb1* induction (Figure S2E), consistent with its reported role as a signature of live bacteria (Moretti et al., 2017). Taken together, these results further demonstrate that excessive c-di-AMP production by *S. aureus* $\Delta thyA$ is responsible for STING activation during infection.

Thymidine availability influences c-di-AMP production by TD-SCVs

Mutations in *thyA* disrupt dTMP (deoxythymidine monophosphate) synthesis from dUMP (deoxyuridine monophosphate), resulting in a reliance on exogenous thymidine to maintain DNA synthesis (Zander et al., 2008). Exogenous thymidine supplementation dampened the IFN- β induction by c-di-AMP producing Firmicutes *L. monocytogenes* (Figure 2B), *E. faecalis* (Figure 2D), and *S. aureus* strains Newman (Figure 2E) and JE2 (Figure 2F) when treated with SXT. As such, we sought to investigate the effect of *thyA* deletion and exogenous thymidine availability on bacterial c-di-AMP production. Supplementation of thymidine restored the growth defect of $\Delta thyA$ in BHI broth in a dose-dependent fashion (Figure 4A). The intracellular c-di-AMP levels of $\Delta thyA$ were comparable with supplementation of 10 µg/mL of thymidine and markedly increased as thymidine levels were decreased (Figure 4B), indicating that thymidine availability regulates c-di-AMP production when *thyA* is inactivated. We quantified the c-di-AMP levels in macrophages

(F) IFN- β concentration in pBMDM supernatants measured by ISRE-luciferase bioassay at 6 hpi.

(G) C-di-AMP levels of NC, $\Delta thyA$, and $\Delta thyA::thyA$ strains quantified by CDA-Luc assay.

(H) *Ifnb1*, *Il6*, *Cxcl10*, and *Ccl5* mRNA induction by NC, $\Delta thyA$, or $\Delta thyA::thyA$ Newman strain in WT or $Sting^{-/-}$ pBMDMs relative to uninfected controls at 4 hpi.

(I) Quantification of c-di-AMP levels of NC, $\Delta thyA$, and *pdeA* overexpression Newman ($\Delta thyA/pdeA$) strains by CDA-Luc assay.

(J) *Ifnb1*, *Il6*, *Cxcl10*, and *Ccl5* mRNA induction in pBMDMs infected with NC, $\Delta thyA$, and $\Delta thyA/pdeA$ strains relative to uninfected control. All infections were performed at an MOI of 20. For all panels, mean values of biological replicates are plotted, and error bars indicate \pm SD. p values were calculated using two-way ANOVA analysis. Asterisks indicate statistical significance (*, p < 0.05; **, p < 0.01; ***, p < 0.001, ****, p < 0.0001), and ns indicates no significant difference.

Cell Host & Microbe

Article

CellPress

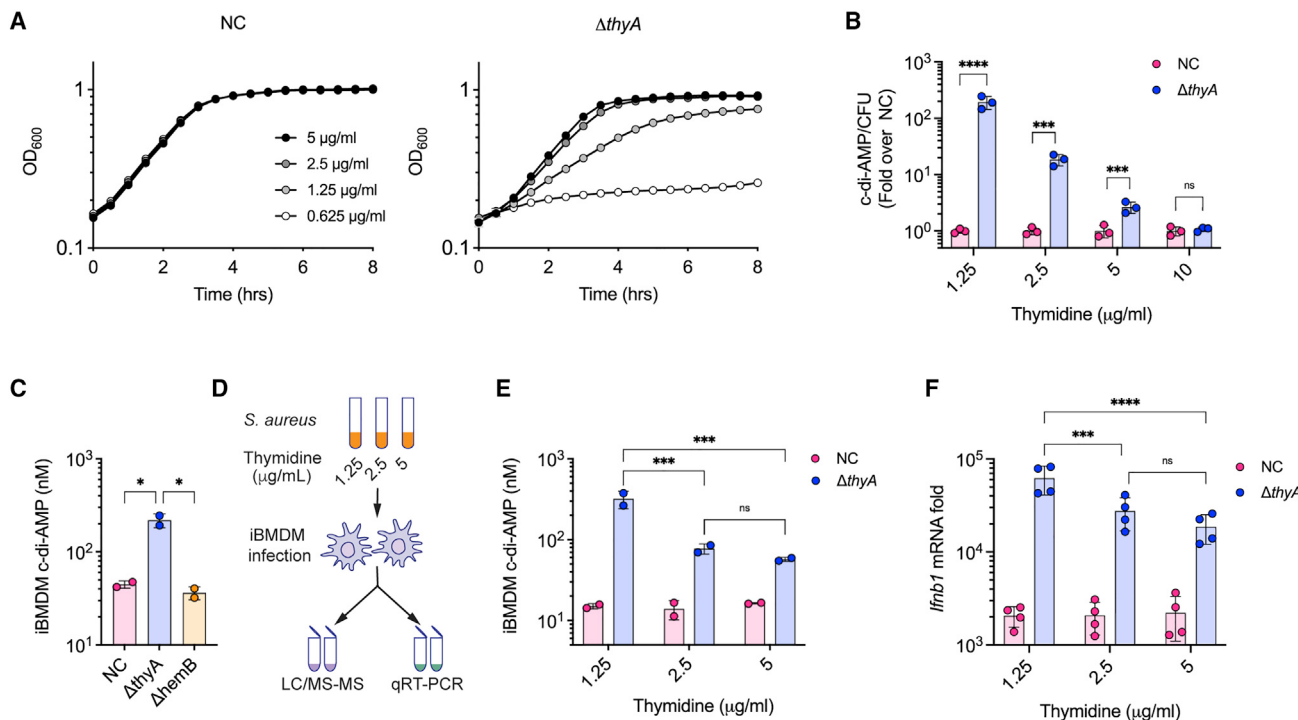


Figure 4. Thymidine abundance modulates c-di-AMP levels and subsequent *Ifnb1* induction of TD-SCV

(A) Growth curve of NC (left) and Δ thyA (right) *S. aureus* Newman in BHI broth supplemented with indicated concentrations of thymidine.

(B) Quantification of c-di-AMP levels of NC and Δ thyA grown in BHI broth supplemented with thymidine by CDA-Luc assay.

(C) LC-MS/MS quantification of intracellular c-di-AMP in iBMDMs infected with NC, Δ thyA, and Δ hemB Newman strains at 4 hpi.

(D) Schematic of macrophage infections. WT iBMDMs were infected with NC or Δ thyA overnight cultures grown in BHI broth supplemented with the indicated thymidine concentrations for 4 h, and the intracellular c-di-AMP levels and *Ifnb1* expression in iBMDMs were determined by LC-MS/MS and qRT-PCR, respectively.

(E and F) The intracellular c-di-AMP concentration (E) and *Ifnb1* mRNA relative to uninfected control (F) as described in (D). All the infections were performed at a MOI of 20. For all panels, mean values of biological replicates are plotted, and error bars indicate \pm SD. p values were calculated using one or two-way ANOVA analysis. Asterisks indicate statistical significance (**, $p < 0.01$; ***, $p < 0.0001$), and ns indicates no significant difference.

infected with logarithmic-phase NC, Δ thyA, or Δ hemB *S. aureus* strains. Consistent with our previous data, macrophages infected with Δ thyA had higher c-di-AMP levels relative to WT- or Δ hemB-infected cells (Figure 4C). We also determined c-di-AMP levels in macrophages infected with Δ thyA or NC strains grown in a range of thymidine concentrations and measured *Ifnb1* mRNA levels in parallel (Figure 4D). Macrophages infected with Δ thyA grown in lower concentrations of thymidine exhibited higher c-di-AMP levels and a correspondingly elevated *Ifnb1* transcriptional response, whereas both c-di-AMP and *Ifnb1* mRNA levels in macrophages infected with NC did not vary when grown in different thymidine concentrations (Figures 4E and 4F). Given that TD-SCV infection leads to higher STING activation than NC *S. aureus* (Figures 3E and 3F), these observations suggest that the STING activation was exacerbated upon thymidine limitation.

c-di-AMP facilitates airway neutrophil infiltration

The association with TD-SCVs and declining lung function among patients with CF is unexpected, given their diminished capacity to survive within host phagocytes and diminished virulence (Kriegeskorte et al., 2014) (Figure S1). Given our findings that elevated c-di-AMP production by TD-SCVs promotes

increased STING-dependent inflammation, we were intrigued to explore the impacts of this pathway in an *in vivo* context. To interrogate the role of c-di-AMP in promoting airway inflammation, we profiled the cytokine levels in the bronchoalveolar lavage fluid (BALF) collected from WT or *Sting*^{-/-} mice following intranasal instillation with the TLR2 agonist Pam3CSK4 either alone or in combination with c-di-AMP. The IRF-3-dependent cytokines CCL5 and CXCL10; the NF κ B-dependent cytokines IL-6, CCL3, CXCL2, and TNF- α were induced by c-di-AMP in a STING-dependent manner (Figure S3; Table S1). The concentrations of top cytokines, IL-6, CXCL10, and CCL5 induced by c-di-AMP were also quantified by ELISA. Induction of these cytokines by Pam3CSK4 and c-di-AMP was found to be both STING and c-di-AMP dependent (Figures 5A–5C). Notably, these cytokines mediate recruitment and activation of neutrophils, the primary innate immune cell type in the defense against *S. aureus* infections (McGuinness et al., 2016), and neutrophil-mediated pulmonary inflammation and injury (Ichikawa et al., 2013; Kaplanski et al., 2003; Pan et al., 2000). Cell counts of the BALF revealed significant c-di-AMP-dependent elevation of neutrophil migration into the airway (Figure 5D).

To confirm if excessive c-di-AMP production in *S. aureus* led to higher inflammation and neutrophil recruitment, a *S. aureus*

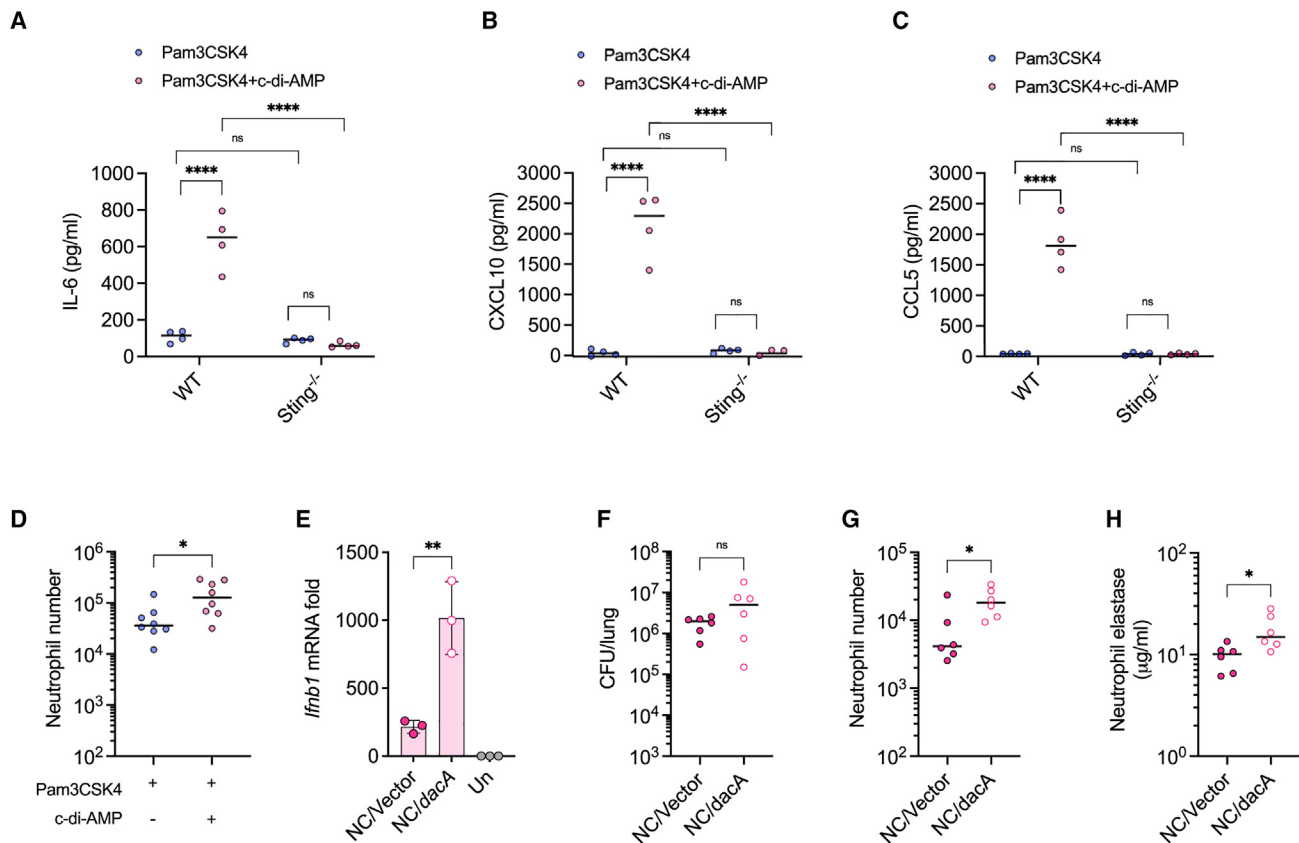


Figure 5. C-di-AMP promotes airway neutrophil infiltration

(A–C) ELISA quantification of cytokines IL-6 (A), CXCL10 (B), and CCL5 (C) in BALF collected from the WT or *Sting*^{-/-} mice intranasally instilled with 15 μg Pam3CSK4 and 15 μg c-di-AMP or Pam3CSK4 alone.

(D) Neutrophil numbers in BALF collected from the WT mice with intranasal instillation of 15 μg Pam3CSK4 and 15 μg c-di-AMP or Pam3CSK4 alone.

(E) *Ifnb1* expression in pBMDMs infected with *dacA* overexpression (NC/*dacA*) and its control (NC/vector) Newman strain relative to uninfected control. Mean values of triplicates are plotted and error bars indicate ±SD. p values were calculated using two-way ANOVA analysis.

(F) CFU recovery from the right lung of WT mice intranasally infected with NC/*dacA* or NC/vector Newman strain at 8 hpi.

(G and H) Neutrophil numbers (G) and active neutrophil elastase concentration (H) in BALF collected from mice infected in (F). Neutrophils are identified and enumerated by FACS. For all the mouse infections, biological replicates are plotted, and horizontal black bars are the median of the data. p values were calculated using Mann-Whitney analysis. Asterisks indicate statistical significance (*, p < 0.05; **, p < 0.01; ***, p < 0.001), and ns indicates no significant difference.

Newman strain ectopically overexpressing the diadenylate cyclase DacA (NC/*dacA*), which synthesizes c-di-AMP (Dengler et al., 2013), was generated. STING activation in macrophages was confirmed along with the control strain (NC/vector) by measuring *Ifnb1* expression (Figure 5E). NC *S. aureus* p:*dacA* exhibited similar bacterial survival relative to control bacteria (Figure 5F) but induced significantly higher neutrophil infiltration and activation as assessed by active elastase concentration in WT mice at 8 hpi (Figures 5G and 5H). This finding establishes that elevated c-di-AMP production is sufficient to promote neutrophil recruitment into the airway during infection.

Airway TD-SCV infection elicits neutrophil infiltration through STING activation

Given that TD-SCVs produce excessive c-di-AMP, we hypothesized that TD-SCV infection could induce airway neutrophil infiltration similar to the effects of c-di-AMP. To investigate this possibility, the clinical TD-SCV isolate 0115-30 was complemented with *thyA* gene because the natural rising clonally

related TD-SCV isolates also possess other mutations in addition to the inactivating mutation of *ThyA* compared with their NC counterparts. As expected, the complementation strain 0115-30::*thyA* failed to induce robust *Ifnb1* expression as 0115-30 in pBMDMs (Figure 6A). WT mice were then intranasally infected with either 0115-30 or 0115-30::*thyA* followed by bronchoalveolar lavage and lung CFU enumeration at 8 hpi. TD-SCV 0115-30 infection resulted in approximately 10-fold lower bacterial recovery than 0115-30::*thyA* from lung tissue in WT mice (Figure 6B). Consistent with the results from c-di-AMP instillation (Figures 5A–C), 0115-30 induced higher production of IL-6, CXCL10, and CCL5 (Figure 6C) and elevated airway neutrophil infiltration (Figure 6D). The neutrophil elastase concentration in BALF, which reflects activated neutrophil levels, was also markedly higher in mice with 0115-30 infection (Figure 6E). These observations establish that clinically derived TD-SCVs are characterized by elevated inflammatory capacity that depends upon disruption of the thymidylate synthase gene.

Cell Host & Microbe

Article

CellPress

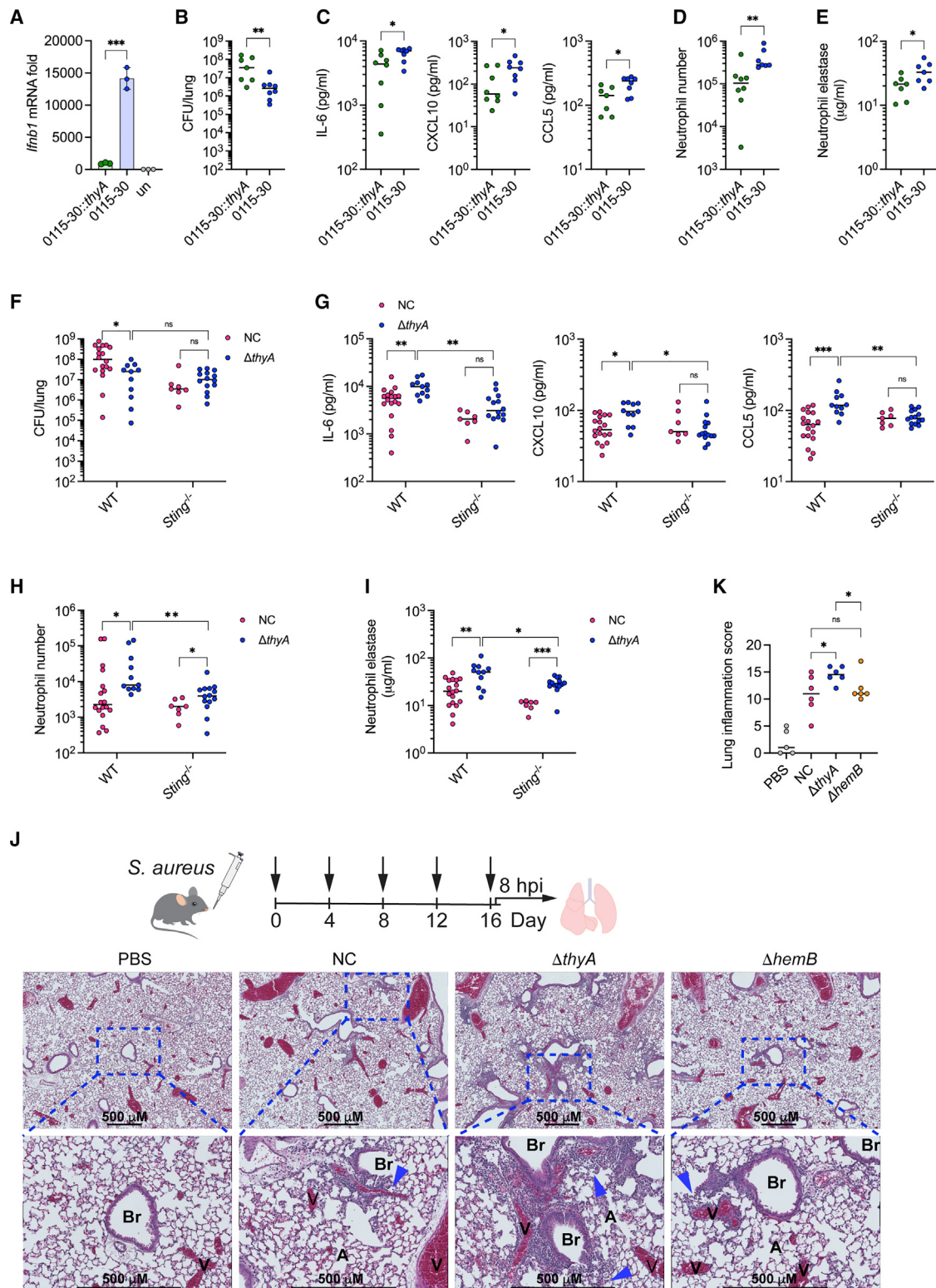


Figure 6. TD-SCVs induce robust airway neutrophil infiltration and inflammation during both acute and recurrent infections

(A) *Ifnb1* expression in pbMDMs infected with 0115-30 or 0115-30::thyA strain relative to uninfected control. Mean values of triplicates are plotted and error bars indicate \pm SD. p values were calculated using two-way ANOVA analysis.

(B) WT mice were intranasally infected with 0115-30 or 0115-30::thyA strains and CFU from the right lung was enumerated at 8 hpi.

(C) ELISA quantification of IL-6, CXCL10, and CCL5 in BALF collected from mice infected in (B).

(legend continued on next page)

To investigate if higher neutrophil induction by TD-SCVs is due to STING activation, WT and *Sting*^{-/-} mice were intranasally infected with either NC or Δ *thyA* *S. aureus* Newman strains. In line with the tissue culture studies (Figure S1A), Δ *thyA* infection resulted in approximately 5-fold lower bacterial recovery from lung tissue in WT mice, whereas *Sting* deletion did not affect the survival of Δ *thyA* (Figure 6F). Δ *thyA* induced significantly higher productions of IL-6, CXCL10, and CCL5 relative to NC in the BALF. Production of the cytokines by Δ *thyA* was significantly decreased in *Sting*^{-/-} mice to levels comparable with those of the NC strain (Figure 6G). Mice infected with Δ *thyA* exhibited significant elevation of airway neutrophil infiltration and neutrophil elastase concentration relative to NC despite the host genotypes; however, *Sting*^{-/-} mice infected with Δ *thyA* demonstrated significantly decreased neutrophil infiltration and elastase concentration (Figures 6H and 6I). Although loss of STING significantly diminished the levels of Δ *thyA*-induced neutrophils and elastase relative to WT mice, a significant increase in these metrics was still observed relative to NC *S. aureus*, supporting increased activation of STING-independent pathways in response to the TD-SCVs. We also revealed that Δ *thyA* was recovered with diminished abundance (Figures S4A and S4B) from lung tissue but induced higher STING-dependent cytokines (Figure S4C), as well as more neutrophil infiltration (Figure S4D), and higher neutrophil elastase activity (Figure S4E) compared with the Δ *hemB* strain. These observations are consistent with elevated c-di-AMP production in Δ *thyA* strains, resulting in STING-dependent inflammation and subsequent neutrophil migration into the airway during lung infection.

Recurrent TD-SCV infection induces higher airway inflammation than other *S. aureus* subtypes

We hypothesized that the hyperinflammatory capacity of TD-SCVs could promote respiratory inflammation in chronic or recurrent infections. To test this, we performed a semiquantitative histopathological analysis of the lungs from mice intranasally instilled with either NC, Δ *thyA*, or Δ *hemB* strains or PBS in a repeat infection model. After five low-dose infections over 16 days, mice infected with all *S. aureus* strains tested exhibited robust airway inflammatory cell infiltration compared with mice treated with PBS (Figure 6J), whereas mice with Δ *thyA* infection exhibited elevated inflammatory cell infiltration and significantly higher inflammation scores relative to the NC and Δ *hemB* strains (Figure 6K; Table S2). These observations establish that despite their diminished capacity to survive *in vivo*, TD-SCVs exhibit elevated inflammatory capacity that promotes immune cell migration to the airway during acute infection. Through charac-

terization of these strains in an animal model that recapitulates recurrent infection, these observations provide an intriguing mechanism for the association of TD-SCVs with worse respiratory outcomes during infections observed in CF.

DISCUSSION

The results of this study demonstrate that disruption of thymidine metabolism results in the elevated production of the second messenger c-di-AMP within several bacterial species, implicating this signaling molecule as a mediator of the stress imposed by thymidine limitation. Our findings also demonstrate that inhibition of thymidine metabolism by commonly used antibiotics significantly increased STING-dependent inflammatory responses following bacterial infection. Additionally, antifolate-resistant thymidine auxotrophs of *S. aureus*, which are frequently isolated from patients with CF and are associated with lower lung function among this patient population (Wolter et al., 2019), similarly exhibit increased STING-dependent inflammation and increased inflammatory cell recruitment into the airway relative to other (less common) SCV types or NC *S. aureus*.

c-di-AMP is a pleiotropic regulator of several key aspects of bacterial physiology, including cell wall synthesis, DNA damage and repair, and osmotic stress responses (Stölke and Krüger, 2020). To date, no link between bacterial c-di-AMP production and thymidine starvation has been reported. Although the molecular mechanism behind this observation remains unresolved, it suggests that c-di-AMP signaling may be involved in countering the stress associated with thymidine limitation. Thymidine depletion is known to induce DNA damage (Besier et al., 2008b), and c-di-AMP signaling has been implicated in the repair of DNA lesions (Oppenheimer-Shaanan et al., 2011). It is therefore tempting to speculate that c-di-AMP levels in TD-SCVs are modulated by pyrimidine metabolism, perhaps through an effect of thymidine starvation on DNA repair pathways.

We also observed elevated production of c-di-AMP in response to β -lactam antibiotics, perhaps reflecting a common role for this CDN in response to diverse antimicrobials. C-di-AMP accumulation inhibits bacterial uptake of potassium and compatible solutes to maintain cellular turgor in response to osmotic stress (Commichau et al., 2018) and osmolarity changes in turn rapidly modulate c-di-AMP metabolism in bacteria (Pham et al., 2018). Modulation of c-di-AMP by *S. aureus* impacts cell size and moderates the effects of extreme membrane and cellwall stress by altering cell size and the composition of the cell wall (Corrigan et al., 2011; Zeden et al., 2018). Because β -lactam antibiotics directly inhibit cell wall biosynthesis,

(D and E) Neutrophil numbers (D) and active neutrophil elastase concentration (E) in BALF collected from mice infected in (B).

(F) WT or *Sting*^{-/-} mice were intranasally infected with NC or Δ *thyA* strain with 5×10^8 CFU/mouse and CFU from the right lung was enumerated at 8 hpi.

(G) ELISA quantification of IL-6, CXCL10, and CCL5 in BALF collected from mice infected in (F).

(H and I) Neutrophil numbers (H) and active neutrophil elastase concentration (I) in BALF collected from mice infected in (F).

(J) Top panel indicates the repeat infection strategy, in which WT mice were intranasally instilled with NC, Δ *thyA*, or Δ *hemB* strain with 2.5×10^7 CFU/mouse or PBS every 4 days for a total of 5 infections. The lungs were harvested 8 h after the last infection. Bottom panel indicates the representative images of H&E staining of WT mouse lung sections. The arrows indicate the inflammatory cell infiltrate. Br, bronchiole; V, blood vessel; and A, alveoli.

(K) Inflammation scoring for mice infected in (J). Inflammation scores were the summation of perivascular/peribronchiolar, intrabronchiolar, intraalveolar, interstitial inflammation, and overall severity. Neutrophils are identified and enumerated by FACS. For all mouse infection panels, biological replicates are plotted. Horizontal black bars indicate the median of the data. p values were calculated using Mann-Whitney analysis. Asterisks indicate statistical significance (*, p < 0.05; **, p < 0.01; ***, p < 0.0001), and ns indicates no significant difference.

elevated c-di-AMP may limit cellular pressure and prevent lysis upon cell wall destabilization. Although links between β -lactams and cellular stability are clear, cellular destabilization is less obvious in the face of thymidine starvation. Cells of ΔthyA *S. aureus* are abnormally shaped during thymidine limitation (Kriegeskorte et al., 2014), and recent findings have indicated a link between cell envelope stability and lytic bacterial death during thymidine limitation (Rao and Kuzminov, 2020). Therefore, c-di-AMP levels may be modulated in response to distorted cellular structure, perhaps by preventing osmolyte accumulation to prevent cellular lysis. Future studies to delineate the molecular mechanism linking c-di-AMP and thymidine starvation will shed significant insight into the role of this second messenger in the physiology of bacteria.

Antibiotic therapy influences the inflammatory properties of bacteria by promoting release of inflammatory components (Orman and English, 2000; Wolf et al., 2017). Proinflammatory effects of antibiotic exposure work in concert with the impacts on microbial growth to clear infection, whereas treatment of infections with high bacterial burdens can promote excessive inflammation and toxic shock. Such processes are most well described for cell wall-targeting antibiotics. Our observations suggest that antifolates may have similar beneficial and detrimental effects depending on the infection context. During acute infections, STING-dependent inflammation may augment the bactericidal activity of these antibiotics in favor of controlling infection. However, STING activation during chronic or recurrent infection contexts may contribute to pathological tissue damage. Our study coupled STING activation with neutrophil infiltration and activation in response to TD-SCV infection in the airway. Neutrophils protect the host against bacterial infection by production of neutrophil extracellular traps (NETs), reactive oxygen and nitrogen species, and antimicrobial proteases and peptides (Porto and Stein, 2016). However, persistent neutrophil recruitment and activation can lead to overexuberant and maladaptive tissue damage (Phillipson and Kubes, 2011). Therefore, chronic inflammatory cell recruitment may damage the airway epithelium and drive lung function decline. Indeed, lung disease is a major complication of the autoimmune disease STING-associated vasculopathy with onset in infancy (SAVI) (Liu et al., 2014), which is caused by STING gain-of-function mutations in humans. Future studies detailing the impacts of STING activation in the context of CF and other infections associated with TD-SCVs may provide new therapeutic interventions to prevent pathology associated with their unique hyperinflammatory properties.

It has not escaped our attention that our data implicate a role for other unique inflammatory properties of the TD-SCV genotype. Specifically, neutrophil infiltration induced by ΔthyA infection is more than 5-fold higher than that with NC or ΔhemB strains, whereas deletion of STING decreased but did not abolish the higher neutrophil infiltration induced by ΔthyA . These observations indicate that TD-SCVs also activate other STING-independent innate immune pathways. TD-SCVs have altered cell wall composition and abnormal cell size (Kahl et al., 2003; Kriegeskorte et al., 2014). This may lead to higher TLR or NOD1/2 activation (Askarian et al., 2018; Brandt et al., 2018), which may also contribute to the hyperinflammatory capacity of TD-SCVs together with STING activation. Although further

work is needed to detail the mechanisms by which TD-SCV impact inflammation during infection, our studies certainly underscore the importance of considering the unique pathologies that may arise during infection with distinct SCV genotypes.

In summary, our study revealed a previously unrecognized impact of thymidine limitation on the production and immune-activating potential of Firmicutes that produce c-di-AMP. We anticipate that the findings of this study will provide insight into the physiological function of the widespread bacterial second messenger c-di-AMP and provide a broader understanding of the impacts of antifolate treatment on the immune response in the context of acute and chronic bacterial infection with bacteria that produce c-di-AMP.

STAR★METHODS

Detailed methods are provided in the online version of this paper and include the following:

- **KEY RESOURCES TABLE**
- **RESOURCE AVAILABILITY**
 - Lead contact
 - Materials availability
 - Data and code availability
- **EXPERIMENTAL MODEL AND SUBJECT DETAILS**
 - Microbe strains and culturing conditions
 - Clinical *S. aureus* SCVs isolation
 - Mice
 - Murine cell lines
- **METHOD DETAILS**
 - Screening of antibiotics that alter bacterial IFN- β induction capacities in pBMDMs
 - Macrophage infection with bacteria
 - Construction of laboratory *S. aureus* SCVs
 - *In vivo* *S. aureus* infection and bacterial burden estimation
 - Repeat infection and histology
 - TaqMan array experiments and relative quantitative real-time PCR
 - Flow cytometry analysis for BAL neutrophils
 - Intranasal c-di-AMP administration
 - Neutrophil elastase assay
 - Quantification of c-di-AMP
- **QUANTIFICATION AND STATISTICAL ANALYSIS**

SUPPLEMENTAL INFORMATION

Supplemental information can be found online at <https://doi.org/10.1016/j.chom.2022.03.028>.

ACKNOWLEDGMENTS

We would like to thank Daniel B. Stetson for providing *Tmem173*^{-/-} and *cGAS*^{-/-} mice and Jessica M. Snyder for histological scoring. We thank Samantha Hopp, Melissa Locke, Chelsea Stamm, and Yaxi Wang for either designing or performing experiments. Q.T. was supported by the University of Washington Cystic Fibrosis Foundation RDP Fellowship (SINGH15R0). This work was supported by a Pilot and Feasibility Award (WOODWA16I0) and a research grant (WOLTER20G0) from the Cystic Fibrosis Foundation and NIH grant R01 AI139071 and AI16669.

AUTHOR CONTRIBUTIONS

Q.T. and J.J.W. conceived and designed the research. Q.T., M.R.P., M.K.T., S.F.B., and F.A.-Q. performed experiments. Q.T., M.K.T., A.P.M., and J.J.W. provided key insights. D.J.W. and L.R.H provided key tools and reagents. Q.T., M.K.T., and J.J.W. analyzed the data and wrote the paper. All authors reviewed the manuscript prior to submission.

DECLARATION OF INTERESTS

The authors declare no competing interests.

Received: September 29, 2021

Revised: February 1, 2022

Accepted: March 23, 2022

Published: April 18, 2022

REFERENCES

- Abe, T., and Barber, G.N. (2014). Cytosolic-DNA-mediated, STING-dependent proinflammatory gene induction necessitates canonical NF- κ B activation through TBK1. *J. Virol.* 88, 5328–5341. <https://doi.org/10.1128/JVI.00037-14>.
- Anderson, R., Tintinger, G., Cockeran, R., Potjo, M., and Feldman, C. (2010). Beneficial and harmful interactions of antibiotics with microbial pathogens and the host innate immune system. *Pharmaceuticals (Basel)* 3, 1694–1710. <https://doi.org/10.3390/ph3051694>.
- Argudín, M.A., Roisin, S., Nienhaus, L., Dodémont, M., de Mendonça, R., Nonhoff, C., Deplano, A., and Denis, O. (2018). Genetic diversity among *Staphylococcus aureus* isolates showing oxacillin and/or cefoxitin resistance not linked to the presence of *mec* genes. *Antimicrob. Agents Chemother.* 62, e00091–18. <https://doi.org/10.1128/AAC.00091-18>.
- Askarian, F., Wagner, T., Johannessen, M., and Nizet, V. (2018). *Staphylococcus aureus* modulation of innate immune responses through Toll-like (TLR), (NOD)-like (NLR) and C-type lectin (CLR) receptors. *FEMS Microbiol. Rev.* 42, 656–671. <https://doi.org/10.1093/femsre/fuy025>.
- Ba, X., Kalmar, L., Hadjirin, N.F., Kerschner, H., Apfalter, P., Morgan, F.J., Paterson, G.K., Girvan, S.L., Zhou, R., Harrison, E.M., and Holmes, M.A. (2019). Truncation of GdpP mediates β -lactam resistance in clinical isolates of *Staphylococcus aureus*. *J. Antimicrob. Chemother.* 74, 1182–1191. <https://doi.org/10.1093/jac/dkz013>.
- Balka, K.R., Louis, C., Saunders, T.L., Smith, A.M., Calleja, D.J., D'Silva, D.B., Moghaddas, F., Tailler, M., Lawlor, K.E., Zhan, Y., et al. (2020). TBK1 and IKK κ act redundantly to mediate STING-induced NF- κ B responses in myeloid cells. *Cell Rep.* 31, 107492. <https://doi.org/10.1016/j.celrep.2020.03.056>.
- Besier, S., Smaczny, C., von Mallinckrodt, C., Krahl, A., Ackermann, H., Brade, V., and Wichelhaus, T.A. (2007). Prevalence and clinical significance of *Staphylococcus aureus* small-colony variants in cystic fibrosis lung disease. *J. Clin. Microbiol.* 45, 168–172. <https://doi.org/10.1128/JCM.01510-06>.
- Besier, S., Zander, J., Kahl, B.C., Kraiczy, P., Brade, V., and Wichelhaus, T.A. (2008b). The thymidine-dependent small-colony-variant phenotype is associated with hypermutability and antibiotic resistance in clinical *Staphylococcus aureus* isolates. *Antimicrob. Agents Chemother.* 52, 2183–2189. <https://doi.org/10.1128/AAC.01395-07>.
- Besier, S., Zander, J., Siegel, E., Saum, S.H., Hunfeld, K.-P., Ehrhart, A., Brade, V., and Wichelhaus, T.A. (2008a). Thymidine-dependent *Staphylococcus aureus* small-colony variants: human pathogens that are relevant not only in cases of cystic fibrosis lung disease. *J. Clin. Microbiol.* 46, 3829–3832. <https://doi.org/10.1128/JCM.01440-08>.
- Brandt, S.L., Putnam, N.E., Cassat, J.E., and Serezani, C.H. (2018). Innate immunity to *Staphylococcus aureus*: evolving paradigms in soft tissue and invasive infections. *J. Immunol.* 200, 3871–3880. <https://doi.org/10.4049/jimmunol.1701574>.
- Brunette, R.L., Young, J.M., Whitley, D.G., Brodsky, I.E., Malik, H.S., and Stetson, D.B. (2012). Extensive evolutionary and functional diversity among mammalian AIM2-like receptors. *J. Exp. Med.* 209, 1969–1983. <https://doi.org/10.1084/jem.20121960>.
- Burdette, D.L., Monroe, K.M., Sotelo-Troha, K., Iwig, J.S., Eckert, B., Hyodo, M., Hayakawa, Y., and Vance, R.E. (2011). STING is a direct innate immune sensor of cyclic di-GMP. *Nature* 478, 515–518. <https://doi.org/10.1038/nature10429>.
- Chen, H., Sun, H., You, F., Sun, W., Zhou, X., Chen, L., Yang, J., Wang, Y., Tang, H., Guan, Y., et al. (2011). Activation of STAT6 by STING is critical for antiviral innate immunity. *Cell* 147, 436–446. <https://doi.org/10.1016/j.cell.2011.09.022>.
- Cheng, Z., Dai, T., He, X., Zhang, Z., Xie, F., Wang, S., Zhang, L., and Zhou, F. (2020). The interactions between cGAS-STING pathway and pathogens. *Signal Transduct. Target. Ther.* 5, 91. <https://doi.org/10.1038/s41392-020-0198-7>.
- Commichau, F.M., Gibhardt, J., Halbedel, S., Gundlach, J., and Stükle, J. (2018). A delicate connection: c-di-AMP affects cell integrity by controlling osmolyte transport. *Trends Microbiol.* 26, 175–185. <https://doi.org/10.1016/j.tim.2017.09.003>.
- Corrigan, R.M., Abbott, J.C., Burhenne, H., Kaever, V., and Gründling, A. (2011). c-di-AMP is a new second messenger in *Staphylococcus aureus* with a role in controlling cell size and envelope stress. *PLoS Pathog.* 7, e1002217. <https://doi.org/10.1371/journal.ppat.1002217>.
- Dengler, V., McCallum, N., Kiefer, P., Christen, P., Patrignani, A., Vorholt, J.A., Berger-Bächi, B., and Senn, M.M. (2013). Mutation in the c-di-AMP cyclase daca affects fitness and resistance of methicillin resistant *Staphylococcus aureus*. *PLoS One* 8, e73512. <https://doi.org/10.1371/journal.pone.0073512>.
- Fernández-Villa, D., Aguilar, M.R., and Rojo, L. (2019). Folic acid antagonists: antimicrobial and immunomodulating mechanisms and applications. *Int. J. Mol. Sci.* 20, 4996. <https://doi.org/10.3390/ijms20204996>.
- Frémond, M.-L., Hadchouel, A., Berteloot, L., Melki, I., Bresson, V., Barnabeï, L., Jeremiah, N., Belot, A., Bondet, V., Brocq, O., et al. (2021). Overview of STING-associated vasculopathy with onset in infancy (SAVI) among 21 patients. *J. Allergy Clin. Immunol. Pract.* 9, 803–818.e11. <https://doi.org/10.1016/j.jaip.2020.11.007>.
- Gaidt, M.M., Ebert, T.S., Chauhan, D., Ramshorn, K., Pinci, F., Zuber, S., O'Duill, F., Schmid-Burgk, J.L., Hoss, F., Buhmann, R., et al. (2017). The DNA inflammasome in human myeloid cells is initiated by a STING-cell death program upstream of NLRP3. *Cell* 171, 1110–1124.e18. <https://doi.org/10.1016/j.cell.2017.09.039>.
- Gao, D., Li, T., Li, X.-D., Chen, X., Li, Q.-Z., Wight-Carter, M., and Chen, Z.J. (2015). Activation of cyclic GMP-AMP synthase by self-DNA causes autoimmune diseases. *Proc. Natl. Acad. Sci. USA* 112, E5699–E5705. <https://doi.org/10.1073/pnas.1516465112>.
- Goerke, C., and Wolz, C. (2010). Adaptation of *Staphylococcus aureus* to the cystic fibrosis lung. *Int. J. Med. Microbiol.* 300, 520–525. <https://doi.org/10.1016/j.ijmm.2010.08.003>.
- Gui, X., Yang, H., Li, T., Tan, X., Shi, P., Li, M., Du, F., and Chen, Z.J. (2019). Autophagy induction via STING trafficking is a primordial function of the cGAS pathway. *Nature* 567, 262–266. <https://doi.org/10.1038/s41586-019-1006-9>.
- Gulen, M.F., Koch, U., Haag, S.M., Schuler, F., Apetoh, L., Villunger, A., Radtke, F., and Ablasser, A. (2017). Signalling strength determines proapoptotic functions of STING. *Nat. Commun.* 8, 427. <https://doi.org/10.1038/s41467-017-00573-w>.
- Hawser, S., Lociuro, S., and Islam, K. (2006). Dihydrofolate reductase inhibitors as antibacterial agents. *Biochem. Pharmacol.* 71, 941–948. <https://doi.org/10.1016/j.bcp.2005.10.052>.
- Huynh, T.N., Luo, S., Pensinger, D., Sauer, J.D., Tong, L., and Woodward, J.J. (2015). An HD-domain phosphodiesterase mediates cooperative hydrolysis of c-di-AMP to affect bacterial growth and virulence. *Proc. Natl. Acad. Sci. USA* 112, E747–E756. <https://doi.org/10.1073/pnas.1416485112>.
- Ichikawa, A., Kuba, K., Morita, M., Chida, S., Tezuka, H., Hara, H., Sasaki, T., Ohteki, T., Ranieri, V.M., dos Santos, C.C., et al. (2013). CXCL10-CXCR3 enhances the development of neutrophil-mediated fulminant lung injury of viral and nonviral origin. *Am. J. Respir. Crit. Care Med.* 187, 65–77. <https://doi.org/10.1164/rccm.201203-0508OC>.

Cell Host & Microbe

Article



- Ishikawa, H., and Barber, G.N. (2008). STING is an endoplasmic reticulum adaptor that facilitates innate immune signalling. *Nature* 455, 674–678. <https://doi.org/10.1038/nature07317>.
- Kahl, B.C., Belling, G., Reichelt, R., Herrmann, M., Proctor, R.A., and Peters, G. (2003). Thymidine-dependent small-colony variants of *Staphylococcus aureus* exhibit gross morphological and ultrastructural changes consistent with impaired cell separation. *J. Clin. Microbiol.* 41, 410–413. <https://doi.org/10.1128/JCM.41.1.410-413.2003>.
- Kaplanski, G., Marin, V., Montero-Julian, F., Mantovani, A., and Farnarier, C. (2003). IL-6: a regulator of the transition from neutrophil to monocyte recruitment during inflammation. *Trends Immunol.* 24, 25–29. [https://doi.org/10.1016/s1471-4906\(02\)00013-3](https://doi.org/10.1016/s1471-4906(02)00013-3).
- Kompis, I.M., Islam, K., and Then, R.L. (2005). DNA and RNA synthesis: antifolates. *Chem. Rev.* 105, 593–620. <https://doi.org/10.1021/cr0301144>.
- Kriegeskorte, A., Block, D., Drescher, M., Windmüller, N., Mellmann, A., Baum, C., Neumann, C., Lorè, N.I., Bragonzi, A., Liebau, E., et al. (2014). Inactivation of *thyA* in *Staphylococcus aureus* attenuates virulence and has a strong impact on metabolism and virulence gene expression. *mBio* 5, e01414–e01447. <https://doi.org/10.1128/mBio.01447-14>.
- Kriegeskorte, A., Lorè, N.I., Bragonzi, A., Riva, C., Kelkenberg, M., Becker, K., Proctor, R.A., Peters, G., and Kahl, B.C. (2015). Thymidine-dependent *Staphylococcus aureus* small-colony variants are induced by trimethoprim-sulfamethoxazole (SXT) and have increased fitness during SXT challenge. *Antimicrob. Agents Chemother.* 59, 7265–7272. <https://doi.org/10.1128/AAC.00742-15>.
- Levdina, H.E., Kelly, K.A., Eshraghi, A., Plemel, R.L., Peterson, S.B., Lee, B., Steele, S., Adler, M., Kawula, T.H., Merz, A.J., et al. (2018). A phosphatidylinositol 3-kinase effector alters phagosomal maturation to promote intracellular growth of *Francisella*. *Cell Host Microbe* 24, 285–295.e8. <https://doi.org/10.1016/j.chom.2018.07.003>.
- Liu, Y., Jesus, A.A., Marrero, B., Yang, D., Ramsey, S.E., Sanchez, G.A.M., Tenbrock, K., Wittkowski, H., Jones, O.Y., Kuehn, H.S., et al. (2014). Activated STING in a vascular and pulmonary syndrome. *N. Engl. J. Med.* 371, 507–518. <https://doi.org/10.1056/NEJMoa1312625>.
- Long, D.R., Wolter, D.J., Lee, M., Precit, M., McLean, K., Holmes, E., Penewitt, K., Waalkes, A., Hoffman, L.R., and Salipante, S.J. (2021). Polyclonality, shared strains, and convergent evolution in chronic cystic fibrosis *Staphylococcus aureus* airway infection. *Am. J. Respir. Crit. Care Med.* 203, 1127–1137. <https://doi.org/10.1164/rccm.202003-0735OC>.
- Ma, Z., and Damania, B. (2016). The cGAS-STING defense pathway and its counteraction by viruses. *Cell Host Microbe* 19, 150–158. <https://doi.org/10.1016/j.chom.2016.01.010>.
- McGuinness, W.A., Kobayashi, S.D., and DeLeo, F.R. (2016). Evasion of neutrophil killing by *Staphylococcus aureus*. *Pathogens* 5, 32. <https://doi.org/10.3390/pathogens5010032>.
- Monk, I.R., Shah, I.M., Xu, M., Tan, M.W., and Foster, T.J. (2012). Transforming the untransformable: application of direct transformation to manipulate genetically *Staphylococcus aureus* and *Staphylococcus epidermidis*. *mBio* 3, e00277–11. <https://doi.org/10.1128/mBio.00277-11>.
- Moretti, J., Roy, S., Bozec, D., Martinez, J., Chapman, J.R., Ueberheide, B., Lamming, D.W., Chen, Z.J., Horng, T., Yeretssian, G., et al. (2017). STING senses microbial viability to orchestrate stress-mediated autophagy of the endoplasmic reticulum. *Cell* 171, 809–823.e13. <https://doi.org/10.1016/j.cell.2017.09.034>.
- Oppenheimer-Shaanan, Y., Wexselblatt, E., Katzhendler, J., Yavin, E., and Ben-Yehuda, S. (2011). c-di-amp reports DNA integrity during sporulation in *Bacillus subtilis*. *EMBO Rep.* 12, 594–601. <https://doi.org/10.1038/embor.2011.77>.
- Orman, K.L., and English, B.K. (2000). Effects of antibiotic class on the macrophage inflammatory response to *Streptococcus pneumoniae*. *J. Infect. Dis.* 182, 1561–1565. <https://doi.org/10.1086/315861>.
- Pan, Z.Z., Parkyn, L., Ray, A., and Ray, P. (2000). Inducible lung-specific expression of RANTES: preferential recruitment of neutrophils. *Am. J. Physiol. Lung Cell. Mol. Physiol.* 279, L658–L666. <https://doi.org/10.1152/ajplung.2000.279.4.L658>.
- Pham, H.T., Nhiep, N.T.H., Vu, T.N.M., Huynh, T.N., Zhu, Y., Huynh, A.L.D., Chakrabortti, A., Marcellin, E., Lo, R., Howard, C.B., et al. (2018). Enhanced uptake of potassium or glycine betaine or export of cyclic-di-AMP restores osmoreistance in a high cyclic-di-AMP *Lactococcus lactis* mutant. *PLoS Genet.* 14, e1007574. <https://doi.org/10.1371/journal.pgen.1007574>.
- Phillipson, M., and Kubes, P. (2011). The neutrophil in vascular inflammation. *Nat. Med.* 17, 1381–1390. <https://doi.org/10.1038/nm.2514>.
- Porto, B.N., and Stein, R.T. (2016). Neutrophil extracellular traps in pulmonary diseases: too much of a good thing? *Front. Immunol.* 7, 311. <https://doi.org/10.3389/fimmu.2016.00311>.
- Precit, M.R., Wolter, D.J., Griffith, A., Emerson, J., Burns, J.L., and Hoffman, L.R. (2016). Optimized *in vitro* antibiotic susceptibility testing method for small-colony variant *Staphylococcus aureus*. *Antimicrob. Agents Chemother.* 60, 1725–1735. <https://doi.org/10.1128/AAC.02330-15>.
- Proctor, R.A., von Eiff, C., Kahl, B.C., Becker, K., McNamara, P., Herrmann, M., and Peters, G. (2006). Small colony variants: a pathogenic form of bacteria that facilitates persistent and recurrent infections. *Nat. Rev. Microbiol.* 4, 295–305. <https://doi.org/10.1038/nrmicro1384>.
- Rao, T.V.P., and Kuzminov, A. (2020). Exopolysaccharide defects cause hyper-thymineless death in *Escherichia coli* via massive loss of chromosomal DNA and cell lysis. *Proc. Natl. Acad. Sci. USA* 117, 33549–33560. <https://doi.org/10.1073/pnas.2012254117>.
- Sauer, J.-D.D., Witte, C.E., Zemansky, J., Hanson, B., Lauer, P., and Portnoy, D.A. (2010). *Listeria monocytogenes* triggers AIM2-mediated pyroptosis upon infrequent bacteriolysis in the macrophage cytosol. *Cell Host Microbe* 7, 412–419. <https://doi.org/10.1016/j.chom.2010.04.004>.
- Smith, S.M., Wunder, M.B., Norris, D.A., and Shellman, Y.G. (2011). A simple protocol for using a LDH-Based cytotoxicity assay to assess the effects of death and growth inhibition at the same time. *PLoS One* 6, e26908. <https://doi.org/10.1371/journal.pone.0026908>.
- Sommer, A., Fuchs, S., Layer, F., Schaudinn, C., Weber, R.E., Richard, H., Erdmann, M.B., Laue, M., Schuster, C.F., Werner, G., and Strommenger, B. (2021). Mutations in the *gdpP* gene are a clinically relevant mechanism for β-lactam resistance in meticillin-resistant *Staphylococcus aureus* lacking *mec* determinants. *Microb. Genomics* 7, 000623. <https://doi.org/10.1099/mgen.0.000623>.
- Stölke, J., and Krüger, L. (2020). Cyclic di-AMP signaling in bacteria. *Annu. Rev. Microbiol.* 74, 159–179. <https://doi.org/10.1146/annurev-micro-020518-115943>.
- Sun, L., Wu, J., Du, F., Chen, X., and Chen, Z.J. (2013). Cyclic GMP-AMP synthase is a cytosolic DNA sensor that activates the type I interferon pathway. *Science* 339, 786–791. <https://doi.org/10.1126/science.1232458>.
- Sun, Y., and Cheng, Y. (2020). STING or Sting: cGAS-STING-mediated immune response to protozoan parasites. *Trends Parasitol.* 36, 773–784. <https://doi.org/10.1016/j.pt.2020.07.001>.
- Topp, S., Reynoso, C.M.K., Seeliger, J.C., Goldlust, I.S., Desai, S.K., Murat, D., Shen, A., Puri, A.W., Komeili, A., Bertozzi, C.R., et al. (2010). Synthetic riboswitches that induce gene expression in diverse bacterial species. *Appl. Environ. Microbiol.* 76, 7881–7884. <https://doi.org/10.1128/AEM.01537-10>.
- Weischenfeldt, J., and Porse, B. (2008). Bone marrow-derived macrophages (BMM): isolation and applications. *CSH Protoc.* 2008. pdb.prot5080. <https://doi.org/10.1101/pdb.prot5080>.
- Whitney, J.C., Peterson, S.B., Kim, J., Pazos, M., Verster, A.J., Radey, M.C., Kulasekara, H.D., Ching, M.Q., Bullen, N.P., Bryant, D., et al. (2017). A broadly distributed toxin family mediates contact-dependent antagonism between gram-positive bacteria. *eLife* 6, e26938. <https://doi.org/10.7554/eLife.26938>.
- Witte, C.E., Whiteley, A.T., Burke, T.P., Sauer, J.D., Portnoy, D.A., and Woodward, J.J. (2013). Cyclic di-AMP is critical for *Listeria monocytogenes* growth, cell wall homeostasis, and establishment of infection. *mBio* 4, e00213–e00282. <https://doi.org/10.1128/mBio.00282-13>.
- Wolf, A.J., Liu, G.Y., and Underhill, D.M. (2017). Inflammatory properties of antibiotic-treated bacteria. *J. Leukoc. Biol.* 101, 127–134. <https://doi.org/10.1189/jlb.4MR0316-153RR>.

- Wolter, D.J., Emerson, J.C., McNamara, S., Buccat, A.M., Qin, X., Cochrane, E., Houston, L.S., Rogers, G.B., Marsh, P., Prehar, K., et al. (2013). *Staphylococcus aureus* small-colony variants are independently associated with worse lung disease in children with cystic fibrosis. *Clin. Infect. Dis.* 57, 384–391. <https://doi.org/10.1093/cid/cit270>.
- Wolter, D.J., Onchiri, F.M., Emerson, J., Precit, M.R., Lee, M., McNamara, S., Nay, L., Blackledge, M., Uluer, A., Orenstein, D.M., et al. (2019). Prevalence and clinical associations of *Staphylococcus aureus* small-colony variant respiratory infection in children with cystic fibrosis (SCVSA): a multicentre, observational study. *Lancet Respir. Med.* 7, 1027–1038. [https://doi.org/10.1016/S2213-2600\(19\)30365-0](https://doi.org/10.1016/S2213-2600(19)30365-0).
- Woodward, J.J., Iavarone, A.T., and Portnoy, D.A. (2010). c-di-AMP secreted by intracellular *Listeria monocytogenes* activates a host type I interferon response. *Science* 328, 1703–1705. <https://doi.org/10.1126/science.1189801>.
- Wu, J., Sun, L., Chen, X., Du, F., Shi, H., Chen, C., and Chen, Z.J. (2013). Cyclic GMP-AMP is an endogenous second messenger in innate immune signaling by cytosolic DNA. *Science* 339, 826–830. <https://doi.org/10.1126/science.1229963>.
- Yin, W., Cai, X., Ma, H., Zhu, L., Zhang, Y., Chou, S.-H., Galperin, M.Y., and He, J. (2020). A decade of research on the second messenger c-di-AMP. *FEMS Microbiol. Rev.* 44, 701–724. <https://doi.org/10.1093/femsre/fuaa019>.
- Yum, S., Li, M., Fang, Y., and Chen, Z.J. (2021). TBK1 recruitment to STING activates both IRF3 and NF- κ B that mediate immune defense against tumors and viral infections. *Proc. Natl. Acad. Sci. USA* 118, e2100225118. <https://doi.org/10.1073/pnas.2100225118>.
- Zander, J., Besier, S., Saum, S.H., Dehghani, F., Loitsch, S., Brade, V., and Wichelhaus, T.A. (2008). Influence of dTMP on the phenotypic appearance and intracellular persistence of *Staphylococcus aureus*. *Infect. Immun.* 76, 1333–1339. <https://doi.org/10.1128/IAI.01075-07>.
- Zaver, S.A., Pollock, A.J., Boradia, V.M., and Woodward, J.J. (2021). A luminescence-based coupled enzyme assay enables high-throughput quantification of the bacterial second messenger 3'3'-cyclic-di-AMP. *ChemBioChem* 22, 1030–1041. <https://doi.org/10.1002/cbic.202000667>.
- Zeden, M.S., Schuster, C.F., Bowman, L., Zhong, Q., Williams, H.D., and Gründling, A. (2018). Cyclic di-adenosine monophosphate (c-di-AMP) is required for osmotic regulation in *Staphylococcus aureus* but dispensable for viability in anaerobic conditions. *J. Biol. Chem.* 293, 3180–3200. <https://doi.org/10.1074/jbc.M117.818716>.
- Zhang, X., Shi, H., Wu, J., Zhang, X., Sun, L., Chen, C., and Chen, Z.J. (2013). Cyclic GMP-AMP containing mixed phosphodiester linkages is an endogenous high-affinity ligand for STING. *Mol. Cell* 51, 226–235. <https://doi.org/10.1016/j.molcel.2013.05.022>.

STAR★METHODS

KEY RESOURCES TABLE

REAGENT or RESOURCE	SOURCE	IDENTIFIER
Antibodies		
Brilliant Violet 421 anti-mouse Ly-6G	BioLegend	Cat# 101319; RRID: AB_1574973
PE/Dazzle 594 anti-mouse/human CD11b	BioLegend	Cat# 101319; RRID: AB_1574973
PerCP/Cyanine5.5 anti-mouse CD45	BioLegend	Cat# 103131; RRID: AB_893344
PE anti-mouse F4/80	BioLegend	Cat# 123109; RRID: AB_893498
TruStain FcX™ PLUS anti-mouse CD16/32	BioLegend	Cat# 101319; RRID: AB_1574973
Bacterial and Virus Strains		
<i>Staphylococcus aureus</i> Newman	Laboratory stock	N/A
<i>Staphylococcus aureus</i> Newman <i>ΔthyA</i>	This paper	N/A
<i>Staphylococcus aureus</i> Newman <i>ΔhemB</i>	This paper	N/A
<i>Staphylococcus aureus</i> Rn4220	Laboratory stock	N/A
<i>Staphylococcus aureus</i> JE2	Laboratory stock	N/A
<i>Staphylococcus aureus</i> Newman <i>ΔthyA::thyA</i>	This paper	N/A
<i>Staphylococcus aureus</i> 0115-30:: <i>thyA</i>	This paper	N/A
<i>Staphylococcus aureus</i> Newman NC/ <i>dacA</i>	This paper	N/A
<i>Staphylococcus aureus</i> Newman <i>ΔthyA::pBAV</i>	This paper	N/A
<i>Staphylococcus aureus</i> Newman NC:: <i>pBAV</i>	This paper	N/A
<i>Staphylococcus aureus</i> Newman <i>ΔthyA/pdeA</i>	This paper	N/A
<i>Staphylococcus aureus</i> Newman NC/ <i>pEPSA5</i>	This paper	N/A
<i>Staphylococcus aureus</i> Newman <i>ΔthyA/pEPSA5</i>	This paper	N/A
<i>Staphylococcus aureus</i> 0115-30 (TD-SCV)	(Wolter et al., 2013)	N/A
<i>Staphylococcus aureus</i> 0115-33 (NC)	(Wolter et al., 2013)	N/A
<i>Staphylococcus aureus</i> 0138-5 (NC)	(Wolter et al., 2013)	N/A
<i>Staphylococcus aureus</i> 0138-11 (TD-SCV)	(Wolter et al., 2013)	N/A
<i>Listeria monocytogenes</i> 10403s	Laboratory stock	N/A
<i>Enterococcus faecalis</i> OG1RF	Laboratory stock	N/A
<i>Salmonella enterica</i> serovar Typhimurium	Laboratory stock	N/A
<i>Francisella novicida</i> U112	(Ledvina et al., 2018)	N/A
<i>Escherichia coli</i> XL1-blue	Agilent Technologies	Cat# 50-125-058
<i>Escherichia coli</i> DH10B	(Monk et al., 2012)	N/A
Chemicals, Peptides, and Recombinant Proteins		
c-di-AMP	Invivogen	Cat# tlrl-nacda
³ H-c-di-AMP	This paper	N/A
MeOSuc-Ala-Ala-Pro-Val-AMC	Cayman	Cat# 14907
Elastase from porcine pancreas	Sigma	SKU# E7885
Critical commercial assays		
TaqMan Gene Expression Master Mix	Applied Biosystems	Cat# 43-695-10
NucleoSpin RNA Plus Kit	Clontech	Cat# 740984.50
iScript cDNA Synthesis Kit	Bio-Rad	Cat# 1708891
TaqMan Array Mouse Immune Panel	Applied Biosystems	Cat# 4367786
Zombie Green™ Fixable Viability Kit	BioLegend	Cat# 423111
Red Cell Lysis Buffer	BioLegend	Cat# 420301
Cell Staining Buffer	BioLegend	Cat# 420201
LDH-Glo Cytotoxicity Assay	Promega	Cat# J2380
Mouse CCL3/MIP-1 alpha Quantikine ELISA Kit	R&D systems	Cat# MMA00

(Continued on next page)

Continued

REAGENT or RESOURCE	SOURCE	IDENTIFIER
Mouse CXCL10/IP-10/CRG-2 DuoSet ELISA	R&D systems	Cat# DY466-05
Mouse CCL5 Quantikine ELISA Kit	R&D systems	Cat# MMR00
Experimental Models: Cell Lines		
Murine: J2 immortalized BMDMs	(Sauer et al., 2010)	N/A
Murine: WT, Tmem173 ^{-/-} , cGAS ^{-/-} primary BMDMs	This paper	N/A
Murine: ISRE-L929 cells	(Woodward et al., 2010)	N/A
Experimental Models: Organisms/Strains		
Mouse: C57BL/6J	The Jackson Laboratory	JAX: 000664
Mouse: C57BL/6J Tmem173 ^{-/-}	(Brunette et al., 2012)	N/A
Mouse: C57BL/6J cGAS ^{-/-}	(Brunette et al., 2012)	N/A
Oligonucleotides		
Mouse <i>Hprt</i> TaqMan probe	Thermo Fisher	Assay ID: Mm03024075_m1
Mouse <i>Ifnb1</i> TaqMan probe	Thermo Fisher	Assay ID: Mm00439552_s1
Mouse <i>Cxcl10</i> TaqMan probe	Thermo Fisher	Assay ID: Mm00445235_m1
Mouse <i>Il6</i> TaqMan probe	Thermo Fisher	Assay ID: Mm00446190_m1
Oligonucleotides used in <i>S. aureus</i> mutant construction	See Table S3	N/A
Oligonucleotides used in construction of <i>dacA</i> or <i>lmpde</i> overexpression vectors	See Table S3	N/A
Oligonucleotides used in mouse genotyping	See Table S3	N/A
Recombinant DNA		
pIMAY	(Monk et al., 2012)	N/A
pIMAY-derivative plasmids	This paper	N/A
pBAV1K-E*	(Topp et al., 2010)	N/A
pBAV1K- <i>thyA</i> expression plasmid	This paper	N/A
pBAV1K-E*- <i>dacA</i> expression plasmid	This paper	N/A
pEPSA5	(Whitney et al., 2017)	N/A
pEPSA5- <i>Lmpde</i> expression plasmid	This paper	N/A
Software and Algorithms		
Prism 6.0	GraphPad	https://www.graphpad.com/scientific-software/prism/ ; RRID:SCR_002798
Morpheus	Broad Institute	https://software.broadinstitute.org/morpheus/ ; RRID:SCR_017386
FlowJo v10.7	FlowJo	https://www.flowjo.com/solutions/flowjo/ ; RRID:SCR_008520
Adobe Photoshop	Adobe	https://www.adobe.com/products/photoshop.html ; RRID:SCR_014199
Adobe Illustrator 2019	Adobe	http://www.adobe.com/products/illustrator.html ; RRID:SCR_010279
Image studio v5.2	LI-COR Biosciences	https://www.licor.com/bio/image-studio-lite/ ; RRID:SCR_015795
Clustal Omega server	Kyoto University Bioinformatics Center	https://www.genome.jp/tools-bin/clustalw
ApE (A plasmid Editor)	M. Wayne Davis	https://jorgensen.biology.utah.edu/wayned/ape/ ; RRID:SCR_014266
Other		
Synergy HTX Multi-Mode Reader	BioTek	N/A
Cytek Aurora	Cytek	N/A
Odyssey Fc Imaging System	LI-COR Biosciences	N/A
CFX Connect Real-Time PCR Detection System	Bio-Rad	Cat# 1855200

(Continued on next page)

Continued

REAGENT or RESOURCE	SOURCE	IDENTIFIER
Tissue-Tearor Homogenizer	BioSpec	Model# 985370-14
Ultrasonic bath sonicator	Fisher Scientific	Model# FS20
Eppendorf Vacufuge Plus	Eppendorf	Model# 5305
Fisherbrand™ Model 505 Sonic Dismembrator	Fisher Scientific	Model# FB505
ViiA 7 Real-Time PCR System	Applied Biosystems	N/A

RESOURCE AVAILABILITY

Lead contact

Please direct any requests for further information or reagents to the lead contact, Joshua J. Woodward (jjwoodwa@uw.edu).

Materials availability

Bacterial strains generated in this study are available from the lead contact upon reasonable request. This study did not generate new unique reagents. Reagents are as described in [key resources table](#).

Data and code availability

- This study did not generate or analyze new datasets.
- This paper does not report original code.
- Any additional information required to reanalyze the data reported in this work paper is available from the Lead Contact upon request.

EXPERIMENTAL MODEL AND SUBJECT DETAILS

Microbe strains and culturing conditions

Clinical *S. aureus* isolates were grown on chocolate II agar (BD, USA). *L. monocytogenes* 10403s, *S. aureus* Newman, *S. aureus* JE2 and *E. faecalis* OG1RF were grown in brain heart infusion (BHI) broth and incubated at 37 °C with shaking. *Escherichia coli* strains used for cloning and *S. typhimurium* SL1344 were grown in Lysogeny broth (LB) at 37 °C with shaking. *F. novicida* was grown in TSBC (30 g tryptic soy broth, 1 g cysteine per liter) at 37 °C with shaking. Hemin-dependent and thymidine-dependent SCVs were grown in BHI broth supplemented with hemin or thymidine at the indicated concentration.

Clinical *S. aureus* SCVs isolation

The clonally related *S. aureus* isolates were obtained retrospectively during a single-center study of children (n=100) with CF ([Wolter et al., 2013](#)). The genetic relatedness of clinical isolates was determined previously using pulse field gel electrophoresis (PFGE) ([Wolter et al., 2013](#)) and whole-genome sequencing (WGS) ([Long et al., 2021](#)). Clonal isolates 0115-30 and 0115-33 differed from one another by 22 nucleotides, specifically, 0115-30 has a 14 bp deletion beginning at position 587 (-GCACTTCCGCCTTG) of the *thyA* gene which results in frameshift mutation and truncation. Isolates 0138-5 and 0138-11 differed by 12 nucleotides, and 0138-11 possesses a missense mutation (C689T) *thyA*, which leads to a Pro230Leu substitution in ThyA ([Figure S5](#)). These 2 groups of isolates were not genetically related to each other by PFGE analysis (< 90% genetic similarity) ([Wolter et al., 2013](#)) or WGS (differed from each other by >20K nucleotides) ([Long et al., 2021](#)).

Mice

All the mice used in this study were in C57BL/6J background. The original breeding pairs of WT were from Jackson Laboratories, cGas^{-/-} and Sting^{-/-} (*Tmem173*^{-/-}) mice were donated by Daniel Stetson at the University of Washington ([Brunette et al., 2012](#)). Mice colonies were bred and maintained under SPF conditions and ensured through the rodent health monitoring program overseen by the Department of Comparative Medicine at the University of Washington. All experiments involving mice were performed in compliance with guidelines set by the American Association for Laboratory Animal Science (AALAS) and were approved by the Institutional Animal Care and Use Committee (IACUC) at the University of Washington. All experiments were carried out with mice aged 8–12 weeks matched by gender, age, and body weight.

Murine cell lines

Primary BMDMs from WT, cGas^{-/-}, and *Tmem173*^{-/-} mice were generated as previously described ([Weischenfeldt and Porse, 2008](#)). The J2 virus immortalized BMDM cell line was from Dan Portnoy at the University of California Berkeley. Both the primary and immortalized BMDMs were cultured were grown at 37 °C in 5% CO₂ in Dulbecco's Modified Eagle Medium (DMEM)

supplemented with 2 mM sodium glutamine, 1 mM sodium pyruvate, 10% heat-inactivated FBS, 0.1% 2-Mercaptoethanol, and 10% L929 cell supernatants as a source of M-CSF.

METHOD DETAILS

Screening of antibiotics that alter bacterial IFN- β induction capacities in pBMDMs

As shown in Figure S6, the screening was performed by the following four steps: 1) Culture of *L. monocytogenes*, a single colony of *L. monocytogenes* 10403s was grown statically in BHI broth at 30 °C overnight to reach the mid-logarithmic phase (OD_{600} 0.8 to 1), the bacterial suspension was diluted with fresh BHI broth to an OD_{600} of 0.25. 2) Antibiotic treatment, 50 μ L of the *L. monocytogenes* suspension was added to each well of the BIOLOG™ microplates (PM11C and PM12B) or a clean 96-well cell suspension plate as an untreated control. The plates were sealed using Breathe-Easy film (Diversified Biotech, USA) to allow the exchange of oxygen and statically incubated at 30 °C for 6 h. The OD_{600} was measured using a Synergy HT microplate reader (BioTek, USA) and the rough CFU was calculated ($CFU/ml = 1.7 \times OD_{600} \times 10^9$). The bacteria suspension was then diluted 1:200 with DMEM medium to dilute the antibiotics. 3) pBMDM infections, 5×10^5 pBMDM cells were seeded in the 96-well tissue culture (TC) plates and incubated at 37 °C in 5% carbon dioxide (CO_2) overnight. 50 μ L of bacteria suspension ($\sim 20 \times 10^5$ CFU) in DMEM medium were then added to the pBMDM cells in duplicates. At 1 hpi, pBMDM supernatants were aspirated and extracellular bacteria were washed off by sterile phosphate-buffered saline (PBS), and the cells were either lysed with 50 μ L H₂O for CFU enumeration or continued incubating in 100 μ L DMEM medium with 50 μ g/mL gentamicin. At 6 hpi, pBMDM supernatants were harvested for downstream IFN- β quantification. 4) IFN- β quantification by ISRE-luciferase assay, 5×10^4 of IFN responsive ISRE-L929 cells (Woodward et al., 2010) were seeded in 96-well TC plates and incubated for 6 h before induction. 25 μ L pBMDM suspensions were added to ISRE-L929 cells and incubated for 12 h. The media was then aspirated, and 50 μ L of TNT lysis buffer (20 mM Tris, 100 mM NaCl, 1% Triton X-100) was added to each well. 40 μ L of the lysate was mixed with 40 μ L of luciferase substrate solution (20 mM Tricine, 2.67 mM MgSO₄·H₂O, 0.1 mM EDTA, 33.3 mM DTT, 530 μ M ATP, 270 μ M acetyl CoA lithium salt, 470 μ M luciferin, 5 mM NaOH, 265 μ M magnesium carbonate hydroxide) and luminescence was measured using a Synergy HT microplate reader (BioTek, USA). The relative ISRE response of each antibiotic treated sample was calculated by the following equation: Relative ISRE response = $[(ISRE\ response)/CFU]/[(ISRE\ response_{untreated\ control})/(CFU_{untreated\ control})]$. For confirmation of the phenotype from the BIOLOG™ microplates, penicillin G, 2,4-Diamino-6,7-diisopropylpteridine, sulfamethoxazole, trimethoprim, SXT (trimethoprim and sulfamethoxazole combination in a 1:5 ratio), and novobiocin was applied in various dilutions to *L. monocytogenes* suspensions.

Macrophage infection with bacteria

For macrophage infection of bacteria treated by SXT, overnight cultures of *L. monocytogenes* 10403s, *E. faecalis* OG1RF, *S. aureus* Newman, *S. aureus* JE2 grown in BHI broth, *F. novicida* grown in TSBC (30 g tryptic soy broth, 1 g cysteine per liter) and *S. typhimurium* SL1344 grown in LB broth were back diluted to OD_{600} of 0.05 and incubated in various concentration of SXT overnight. 1×10^6 of pBMDMs were plated in 6-well tissue culture plates and incubated at 37 °C in 5% carbon dioxide (CO_2) overnight. Bacteria were washed with sterile phosphate-buffered saline (PBS) and then re-suspended in DMEM medium. The macrophages were infected by *L. monocytogenes* at a MOI of 4, *S. aureus* at a MOI of 20, *S. typhimurium* at a MOI of 1. After a 1 hr incubation, the cells infected with *L. monocytogenes* and *S. typhimurium* were washed once with PBS and given fresh DMEM medium containing 50 μ g/ml gentamicin to kill the extracellular bacteria. The cells infected with *S. aureus* strains were washed once with PBS and given fresh DMEM medium containing 100 μ g/ml gentamicin. At 4 hpi, cells were collected for RNA isolation. For macrophage infection with *F. novicida*, pBMDMs were infected with *F. novicida* at a MOI of 100. After 4 hpi, the cells were washed once with PBS and given fresh DMEM medium containing 50 μ g/ml gentamicin, and the cells were collected at 6 hpi for RNA isolation.

For the study of the inflammatory capacity or intracellular survival of *S. aureus*, either 1×10^6 iBMDM or pBMDMs were plated in 6-well tissue culture plates and incubated at 37 °C in 5% carbon dioxide (CO_2) overnight. Mid-exponential phase *S. aureus* cultures were washed once with sterile PBS and then re-suspended in DMEM medium. The macrophages were infected by *S. aureus* at a multiplicity of infection of 20 or 100. After a 1 hr incubation, the cells were washed twice with PBS and given fresh DMEM medium containing 100 μ g/ml gentamicin to kill the extracellular bacteria. At various times post-infection, supernatants were collected to study macrophage cell death by lactate dehydrogenase (LDH) release assays (Promega, USA) (Smith et al., 2011), IFN- β protein expression by luciferase bioassays (Woodward et al., 2010), and cells were collected for RNA isolation. For the luciferase bioassay, supernatants were applied in various dilutions to the IFN responsive ISRE-L929 cells (5×10^4 cells/well, 96-well plate). The cells were lysed by TNT lysis and added to luciferase substrate solution and luminescence was measured using a Synergy HT (BioTek, USA). For intracellular CFU enumeration, macrophages were lysed by adding H₂O and incubating at 37 °C for 5 min. Appropriate dilutions were plated on BHI agar plates and incubated at 37 °C overnight and CFU were enumerated.

Construction of laboratory *S. aureus* SCVs

S. aureus Newman $\Delta thyA$ and $\Delta hemB$ strains were constructed by allelic exchange using pIMAY (Monk et al., 2012). Briefly, primers were designed to amplify upstream and downstream regions flanking the gene(s) of interest (either *thyA* or *hemB*) to delete the entire open reading frame (Table S2). Genomic DNA from *S. aureus* strain Newman was used as a template to generate fragments consisting of linked sequences upstream and downstream of either *thyA* or *hemB* ($\Delta thyA$ or $\Delta hemB$ cassette) by overlapping PCR. The deletion cassette was cloned into pIMAY and transformed into *E. coli* DH10B and then transformed into *S. aureus* strain RN4220.

via electroporation. Transduction of *S. aureus* strain Newman was accomplished by first propagating phage φ-11 (to package the pIMAY vector) in RN4220 that had been successfully transformed with the pIMAY_deletion cassette ($\Delta thyA$ or $\Delta hemB$). Allelic exchange of either $\Delta thyA$ or $\Delta hemB$ was achieved by subsequent generalized phage transduction of the appropriate φ-11 pIMAY_deletion cassette vector into strain Newman. The resulting SCV strains were confirmed by PCR and further tested for auxotrophy for either thymidine or hemin; both showed attenuated growth in vitro compared with the wild-type Newman strain in the absence of either thymidine or hemin.

The *dacA* overexpression strain (NC/*dacA*) was constructed by electroporation of a pBAV1K-E* plasmid (Topp et al., 2010) expressing the *S. aureus* *dacA* gene driven by a theophylline-inducible riboswitch into the *S. aureus* Newman strain. 1 mM theophylline was supplemented to induce the expression of *dacA*. The complementation strain 0115-30::*thyA* and $\Delta thyA$::*thyA* were constructed by electroporation of a pBAV1K-E* plasmid backbone carrying *thyA* gene and its original promoter to 0115-30 or $\Delta thyA$ strain, respectively. The empty pBAV1K-E* plasmid was electroporated to the NC and $\Delta thyA$ strains to construct the control strains NC::pBAV and $\Delta thyA$::pBAV, respectively. The *pdeA* overexpression strain ($\Delta thyA$ /*pdeA*) was constructed by electroporation of pEPSA5 plasmid (Whitney et al., 2017) expressing the cytosol soluble fragment of *L. monocytogenes* 10430s phosphodiesterase PdeA₈₄₋₆₈₇ into the $\Delta thyA$ strain. The empty pEPSA5 plasmid was transferred to the NC and $\Delta thyA$ strains to construct the control strains NC/pEPSA5 and $\Delta thyA$ /pEPSA5, respectively. 2% xylose was supplemented to induce the expression of *pdeA*.

In vivo *S. aureus* infection and bacterial burden estimation

Mice aged 8–12 weeks were used in infection experiments. Prior to animal experiments, overnight cultures of NC, $\Delta thyA$ and $\Delta hemB$ were back diluted twice ($OD_{600}=0.15$) and grown for 2 h at 37 °C with 5 µg/mL of thymidine and 1 µg/mL hemin in BHI broth, respectively, to reach mid-exponential growth. Subsequently, the bacteria were washed once with cold PBS. Cultures were diluted in 30 µL PBS to achieve a final inoculum of 5×10^8 CFU/mouse and used to infect mice via the intranasal route while the animals were anesthetized with isoflurane. Mice were euthanized and lungs collected at the indicated time points. Lungs were homogenized and lysed in 5 mL PBS using a Tissue Tearor Homogenizer. Bacterial burdens were enumerated by plating dilutions on BHI plates containing thymidine or hemin to ensure the normal growth of SCVs.

Repeat infection and histology

Mice aged 8–12 weeks were either intranasally instilled with 2.5×10^7 bacteria in 30 µL PBS or 30 µL PBS every 4 days for a total of 5 infections. On day 16, mice were euthanized by CO₂ exposure, the lungs were inflated with 1 mL cold 4% formalin and the trachea were tied up using silk string. Whole lungs were immersion fixed in 4% formalin, paraffin embedded, sectioned, stained with hematoxylin and eosin (H&E) and then evaluated for lung inflammation and injury. Lungs were scored semi-quantitatively in a blinded fashion for lung inflammation which includes perivascular/peribronchiolar inflammation, intrabronchiolar inflammation, interstitial inflammation, intraalveolar inflammation and severity/extent using a 1–4 scale in which 1 through 4 generally indicated “minimal”, “mild”, “moderate”, and “severe” changes, respectively. The representative images were scanned by Keyence BZ-X710 microscope and image brightness and contrast were adjusted using Photoshop applied to the entire image. Original magnification was as stated.

TaqMan array experiments and relative quantitative real-time PCR

RNA from the macrophages was isolated using NucleoSpin RNA Plus Kit (Clontech, USA) followed by cDNA synthesis using iScript cDNA synthesis Kits (Bio-Rad, USA) following manufacturer’s instructions. qRT-PCR was performed using TaqMan Gene expression master mix (Thermo Fisher Scientific, USA). Taqman probes for mouse genes were pre-designed from Thermo Fisher Scientific. To calculate mRNA fold change, transcript levels were determined by normalizing to mouse *Hprt* using the $2^{(-\Delta\Delta Ct)}$ method. Immune gene expression profiling was performed using TaqMan Array Micro Fluidic Cards (Applied Biosystems, USA) containing probe sets for 90 immune genes and 6 endogenous controls.

Flow cytometry analysis for BAL neutrophils

Mice were euthanized at the indicated time by CO₂ asphyxiation and lungs were lavaged with 0.5 ml ice-cold PBS twice. A total of 1 mL of lavage fluid was centrifuged at 2,000 g for 2 min. Collected cells were resuspended in 100 µL Red Cell Lysis Buffer (BioLegend, USA) and incubated for 5 min. Cell lysis was stopped by adding 400 µL Cell Staining Buffer (BioLegend, USA). Cells were then centrifuged at 2,000 g for 2 min and re-suspend in the Cell Staining Buffer. Viable cells were counted using the Automatic cell counter (Bio-Rad) after trypan blue staining. Fc receptors were blocked by incubating cells with TruStain FcX™ PLUS anti-mouse CD16/32 antibody (Biolegend, USA) for 10 min. Cells were stained using the Zombie Green Fixable Viability Kit (BioLegend, USA) for 10 min to detect dead cells. Cells were washed twice with 500 µL PBS and resuspended in the Cell Staining Buffer (BioLegend, USA). Cells were thereafter stained with antibodies for the desired surface markers for 20 min on ice in the dark. Flow cytometric data were acquired on Cytek Aurora and analyzed using the FlowJo software. The following antibodies specific for the cell surface antigens from Biolegend were used for the flow cytometry: Brilliant Violet 421 anti-mouse Ly-6G, PE/Dazzle 594 anti-mouse/human CD11b, PerCP/Cyanine5.5 anti-mouse CD45, PE anti-mouse F4/80. 10,000 live singlet cells were pre-gated. Neutrophils were identified as live, CD45⁺, F4/80⁺, CD11b⁺, Ly6G⁺. The neutrophil numbers were calculated according to total cells in BALF and the percent of neutrophil identified by FACS assay.

Intranasal c-di-AMP administration

C57BL/6J WT or *Sting*^{-/-} mice aged 8–12 weeks were anesthetized under isoflurane. Mice were intranasally instilled with either 30 µL PBS, PBS containing 15 µg c-di-AMP and 15 µg Pam3CSK4, or PBS containing 15 µg Pam3CSK4 and sacrificed at 8 h after treatment for BAL. The neutrophil numbers in BALF were enumerated by FACS assay and CXCL10, CCL5 and IL-6 concentrations in the BALF were measured by using the Mouse Quantikine ELISA Kit (R&D, USA).

Neutrophil elastase assay

Elastase activity was measured by spectrofluorometrically monitoring the hydrolysis product of the fluorogenic substrate MeOSuc-AAPV-AMC (Cayman, USA). BALF was centrifuged at the maximum speed to remove the cell debris, then 20 µL BALF was mixed with 80 µL substrate solution (0.1 mM MeOSuc-AAPV-AMC, 0.5 M NaCl, 0.01 M CaCl₂, 10% DMSO, 0.05 M Tris, pH 7.5) in white bottom 96-well plates. The kinetics of substrate cleavage (increase in fluorescence of the liberated 7-amino-4-methylcoumarin, AMC) was measured using a fluorometer (BioTek, USA) set at 370 nm excitation and 460 nm emission at 37°C. Porcine elastase (Sigma, USA) was used to generate a standard curve.

Quantification of c-di-AMP

The intercellular c-di-AMP of *S. aureus* strains was extracted by methanol and quantified by either LC-MS ([Huynh et al., 2015](#)) or luminescence-based coupled enzyme assay for c-di-AMP quantification (CDA-Luc) ([Zaver et al., 2021](#)) as previously described. Briefly, overnight culture of *S. aureus* strains grown in BHI supplemented with 5 µg/mL of thymidine were washed twice by PBS, then diluted into fresh BHI containing various concentrations of thymidine (1.25, 2.5, 5, and 10 µg/mL) with the initial OD₆₀₀ of 0.05, and grown at 37 °C with shaking to reach logarithmic phase (OD₆₀₀ around 0.8). The bacteria were collected by centrifugation (15,000 × g, 5 min) and used for c-di-AMP extraction or iBMDM infection. Macrophages infected with bacteria were collected by incubating in 0.05% Trypsin-EDTA for 5 min. Cells were then re-suspended in 500 µL methanol and lysed in an ultrasonic bath sonicator for 5 min (Fisher Scientific, USA); Bacteria were re-suspended in 500 µL methanol and lysed by sonication with 40% setting for 5 pulses (1 second on/1 second off) (Fisher Scientific, USA). For quantification of c-di-AMP using LC-MS, heavy-labeled (³H) c-di-AMP was added into the extract as the internal control. Bacterial lysates were centrifuged to collect cell-free supernatants. The methanol extracts containing c-di-AMP were dried overnight in a vacufuge (Eppendorf, USA), and re-suspended in water for c-di-AMP quantification by LC-MS as previously described ([Huynh et al., 2015](#)). For quantification of intercellular c-di-AMP of *S. aureus* using CDA-Luc, the methanol extracts were re-suspended in ice-cold pull-down buffer (100 µM Tris pH 7.5, 20 mM MgCl₂, 50 mM NaCl) and c-di-AMP quantified as previously described ([Zaver et al., 2021](#)). The intercellular c-di-AMP of *L. monocytogenes* strains was quantified by CDA-Luc as previously described ([Zaver et al., 2021](#)). Briefly, the overnight culture of *L. monocytogenes* grown statically at 30 °C was collected by centrifugation. The bacterial pellets were re-suspended with pull-down buffer and lysed by sonication for c-di-AMP quantification ([Zaver et al., 2021](#)).

QUANTIFICATION AND STATISTICAL ANALYSIS

All numerical data were analyzed and plotted using GraphPad Prism 6.0 software. For all the tissue culture and c-di-AMP quantification plots, mean values of biological replicates are plotted, and error bars indicate ±SD; data shown in animal infection plots are represented as the median of biological replicates. The exact numbers of replicates are stated in the figures. Statistical tests used and statistical parameters for each experiment are enclosed in their respective figure legends. No methods were used to determine whether the data met assumptions of the statistical approach.